The dynamic surface proteomes of allergenic fungal conidia

Matthew G. Blango[1], Annica Pschibul[1,2], Flora Rivieccio[1], Thomas Krüger[1], Muhammad Rafiq[1,2], Lei-Jie Jia[1], Tingting Zheng[3], Marie Goldmann[1,2], Vera Voltersen[1], Jun Li[4,5], Gianni Panagiotou[3], Olaf Kniemeyer[1,2]*, Axel A. Brakhage[1,2]*

[1] Department of Molecular and Applied Microbiology, Leibniz Institute for Natural Product Research and Infection Biology—Hans Knöll Institute (Leibniz-HKI), Jena, Germany.

[2] Department of Microbiology and Molecular Biology, Institute of Microbiology, Friedrich Schiller University, Jena, Germany.

[3] Department of Systems Biology and Bioinformatics, Leibniz Institute for Natural Product Research and Infection Biology—Hans Knöll Institute (Leibniz-HKI), Jena, Germany.

[4] Department of Infectious Diseases and Public Health, Jockey Club College of Veterinary Medicine and Life Sciences, City University of Hong Kong, Hong Kong S.A.R., China

[5] School of Data Science, City University of Hong Kong, Hong Kong S.A.R., China

Running Title: Surface proteome of fungal conidia

Key Words: *Aspergillus fumigatus*, *Alternaria alternata*, *Penicillium rubens*, *Cladosporium herbarum*, proteome, germling, hyphae, LC-MS/MS, secreted proteins

*Correspondence:

E-mail olaf.kniemeyer@leibniz-hki.de; Tel. +49 (0)3641-532 1071

E-mail axel.brakhage@leibniz-hki.de; Tel. +49 (0)3641-532 1001.

Abstract

Fungal spores and hyphal fragments are major contributors to the allergic response in the human lung. In this study, we used a trypsin-shaving-proteomics approach to identify the surface-exposed and secreted/shed proteins of *Aspergillus fumigatus* conidia. We investigated the surface proteome under different conditions, including temperature variation and germination. We found that the surface proteome of resting *A. fumigatus* conidia is not static, but instead unexpectedly dynamic, as evidenced by drastically different surface proteomes under different growth conditions. Knockouts of two abundant *A. fumigatus* surface proteins, ScwA and CweA, were found to function only in fine-tuning the cell wall stress response, implying that the conidial surface is also very robust. We then compared the surface proteome of *A. fumigatus* to other allergy-inducing molds, including *Alternaria alternata*, *Penicillium rubens,* and *Cladosporium herbarum,* and performed comparative proteomics on resting and swollen conidia, as well as secreted proteins from germinating conidia. We detected 125 protein ortholog groups, including 80 with putative catalytic activity, in the extracellular region of all four molds, and 42 nonorthologous proteins produced solely by *A. fumigatus*. Ultimately, this study highlights the dynamic nature of the conidial surface and provides numerous targets for future diagnostics and immunotherapy.

Introduction

120,000 fungal species have been described to date; however, only a few hundred of these fungi are able to cause illness in humans [1]. These diseases range from mild allergic reactions to life-threatening systemic infection. In terms of allergy, more than 80 mold genera have been associated with hypersensitive responses in allergic patients [2]. Within this group, species of the genera *Alternaria* and *Cladosporium* represent the most

49 important outdoor allergens, while species of *Penicillium* and *Aspergillus* are reported to be the most common
50 indoor airborne fungi [3]. *A. fumigatus* is associated with different forms of allergic diseases, including allergic
51 bronchopulmonary aspergillosis (ABPA; [4]), a persistent colonization of the bronchi known to frequently occur
52 in patients with asthma and cystic fibrosis. In addition, *A. fumigatus* is the most common species within the
53 mold fungi to cause invasive infections in the lungs of immunocompromised patients, which is designated
54 invasive aspergillosis.

55 The *A. fumigatus* infectious lifecycle starts with the inhalation of conidia, 2-3 µm asexual spores,
56 produced by mature conidiophores [5]. After deposition in the lungs, conidia undergo germination, whereby
57 they initially swell, extend germ tubes, and finally form hyphae [6]. The small size and ubiquitous nature of these
58 fungal spores requires that the human innate immune system must continuously defend against inhaled conidia.
59 Epithelial cells are the likely source of first contact in the mammalian lung, but recruitment of alveolar
60 macrophages and neutrophils quickly follows [7]. Recognition by macrophages typically results in phagocytosis
61 of conidia, while recruitment of neutrophils provides an additional level of antifungal defense [8]. In
62 immunocompromised patients, specifically those with neutropenia, these host defenses are impaired and result
63 in unregulated fungal growth with dangerous clinical manifestations [9]. Far less is known about the adaptive
64 immune response to *A. fumigatus*, but it has recently been demonstrated that tolerance to inhaled conidia is
65 mainly mediated by antigen-specific FOXP3+ regulatory T cells [10].

66 In addition to *Aspergilli*, species of *Alternaria*, *Cladosporium*, and *Penicillium* are among the most
67 commonly inhaled ascomycete molds capable of causing allergic diseases in humans [2, 11]. Organisms in the
68 genus *Penicillium* are genetically closely related to the *Aspergilli* and exhibit similar lifecycles; however,
69 *Penicillium* species rarely cause infectious disease, but rather asthma and allergic rhinitis in adults and children
70 [12]. *Alternaria* and *Cladosporium* species are a major source of disease in plants, but they also represent
71 important environmental allergens associated with asthma and asthma exacerbations [3]. Due to their
72 abundance in nature, it is not surprising that conidia and/or hyphal fragments containing immune-activating

73 allergenic proteins from these fungi are thought to be a major source of fungal-induced allergy [13]. Many
74 allergens have been identified from each organism, with *A. fumigatus* containing >40 known allergen proteins
75 [2, 14], and *A. alternata*, *C. herbarum*, and *P. chrysogenum* (*rubens*) ranging from 6-17 protein antigens. Despite
76 this knowledge of allergens, our understanding of the complex interplay between fungus and host remains
77 limited. The protein, lipid, and carbohydrate composition of a conidium has a direct impact on its recognition by
78 the immune system and the following response of either tolerance or inflammation [5].

79 The conidium of *A. fumigatus* is the best studied mold spore to date [15]. Previous studies have
80 elucidated the cell wall and surface proteome of *A. fumigatus* conidia to understand the molecules that likely
81 interact with the host [16-18]. Throughout germination the surface of the fungi changes dramatically, in terms of
82 both the cell wall proteome and carbohydrate organization [19, 20]. One major protein on the surface of conidia
83 is the RodA hydrophobin, which encases resting conidia in a hydrophobic coat to minimize interactions with
84 potential hazards. This hydrophobic rodlet layer is composed of a regular arrangement of the RodA protein
85 interwoven amongst a layer of dihydroxynaphthalene (DHN)-melanin pigment. Upon encountering favorable
86 growth conditions, resting conidia begin germination; a process that is highlighted by disassembly of the rodlet
87 layer and degradation of the DHN-melanin polymer [21-23]. Despite this key function, RodA is not required for
88 virulence in mammalian infection models [22]. Aside from RodA, the functions of few other *A. fumigatus*
89 surface-exposed proteins are known. In many cases, these proteins seem to play important, but enigmatic roles
90 in fungal biology, as is the case with the recently described CcpA protein, which serves as a conidial protein
91 important for virulence in a mouse infection model [16]. CcpA appears to serve a structural role that normally
92 masks other antigenic proteins in the conidial cell wall. Despite our increasing understanding of the biology of
93 fungal conidia, our ability to rapidly detect, diagnose, and treat fungal pathogens remains limited [24]. As the
94 burden of fungal pathogens in the clinic increases, improvements in each of these realms are desperately
95 needed. [25]

96 In this study we further elucidated the surface-exposed proteome and secreted/shed proteins of allergy-
97 inducing fungal conidia to reveal new fungal surface antigens as potential diagnostic targets. In addition,
98 similarities and differences between the mold species were discovered, as well as the influence of
99 environmental factors like temperature on the composition of the conidial surface proteome. We also focused
100 on the biology of two particularly abundant, previously uncharacterized cell wall proteins of *A. fumigatus*,
101 Afu4g09600 and Afu4g09310, which are denoted here as "Cell Wall Enriched A" (CweA) and "Small Cell Wall
102 Peptide A" (ScwA), respectively.
103

104 **Materials and Methods**

105 **Fungal strains and cultivation.** All strains used in this study are listed in **Table S1**. Cultivation of *A. alternata*
106 (Fries) Keissler (ATCC 66981), *P. rubens* WIS 54-1255 (ATCC 28089; formerly *P. chrysogenum WIS 54-1255*), and
107 *A. fumigatus* CEA10 was performed on *Aspergillus* minimal medium (AMM; 70 mM $NaNO_3$, 11.2 mM KH_2PO_4, 7
108 mM KCl, 2 mM $MgSO_4$, and 1 µl/ml trace element solution (pH 6.5)) agar plates with 1% (w/v) glucose at room
109 temperature for the comparative analysis. The trace element solution was composed of 1 g $FeSO_4 \bullet 7\ H_2O$, 8.8 g
110 $ZnSO_4 \bullet 7\ H_2O$, 0.4 g $CuSO_4 \bullet 5\ H_2O$, 0.15 g $MnSO_4 \bullet H_2O$, 0.1 g $NaB_4O_7 \bullet 10\ H_2O$, 0.05 g $(NH_4)_6Mo_7O_{24} \bullet 4\ H_2O$,
111 and ultra-filtrated water to 1000 ml [26, 27]. *C. herbarum* Link: Fries (ATCC MYA-4682) was cultivated on malt
112 agar plates for 7 days at room temperature for the comparative analysis as AMM was not a permissible growth
113 condition. All conidia were harvested in sterile, ultra-filtrated water. ~$1x10^9$ resting conidia were used
114 immediately after collection for trypsin shaving. For germination, >$1x10^9$ *A. fumigatus* resting conidia grown for
115 7 days at 37°C were germinated shaking in RPMI 1640 (Lonza) supplemented with glucose to a final
116 concentration of 2% (w/v) at 37°C to produce swollen conidia (5 h), germlings (8 h), and hyphae (14 h).
117

118 **Extraction of surface proteins by trypsin shaving.** Surface proteins were extracted as described previously [16].
119 Briefly, resting conidia, swollen conidia, germlings, and/or hyphae of *A. fumigatus*, *A. alternata*, *C. herbarum*,

120 and *P. rubens* were each washed twice with 25 mM ammonium bicarbonate and collected by centrifugation
121 (1,800 × *g* for 10 min at room temperature). Samples were resuspended in 800 µl of 25 mM ammonium
122 bicarbonate and treated with 5 µg trypsin (Serva) for 5 min at 37°C with gentle agitation. Samples were then
123 immediately passed through a 0.2 µm cellulose acetate filter (Sartorius) and collected in a microcentrifuge tube,
124 followed by washing of the syringe with 200 µl of 25 mM ammonium bicarbonate. 9 µl of 89% (v/v) formic acid
125 was added to stop the tryptic digestion. The samples were dried using a SpeedVac Concentrator (Thermo-
126 Fisher), resuspended in 25 µl of 2% (v/v) ACN and 0.05% (v/v) TFA, and centrifuged for 15 min through a 10 kDa
127 cutoff microfuge column (VWR Scientific). Conidia were collected after trypsin treatment and tested for lysis
128 using a brief (15 min) staining with 40 µM propidium iodide followed by imaging with a Zeiss Axio Imager.M2
129 microscope (Zeiss). In some instances, the 10 kDa cutoff centrifugation step was replaced with centrifugation
130 through a 0.22-µm-pore-size Spin X cellulose acetate spin filter (Corning Costar).
131
132 **Purification of secreted proteins from swollen conidia.** For the identification of secreted proteins, ~$2x10^9$
133 resting conidia were germinated as described above for 5 h, before collection of the supernatant by filtration
134 through a 0.22 µm filter and addition of TFA to a final concentration of 0.1% (v/v). Protein was purified by SPE
135 with a Chromabond SPE-C4 cartridge (Macherey-Nagel, Germany). Briefly, columns were washed with 4 mL
136 methanol and reconstituted with 4 mL 0.1% (v/v) TFA. Sample supernatants were aspirated through columns,
137 washed with 2 mL 5% (v/v) MeOH / 0.1% (v/v) TFA, and eluted in 4 mL 0.1% (v/v) TFA 80/10 ACN/H_2O (v/v).
138 Samples were then dried by SpeedVac, resolubilized in 100 µL denaturation buffer (50 mM triethylammonium
139 bicarbonate (TEAB) in 50/50 trifluoroethanol (TFE)/H_2O (v/v)), sonicated for 15 min, and homogenized by Vortex
140 mixing. Following 10 min at 90°C, samples were collected by centrifugation and cooled on ice. Protein content
141 was measured with a Merck Millipore Direct Detect spectrometer. The samples were then reduced by adding
142 2 µL of reduction buffer (500 mM tris(2-carboxyethyl)phosphine in 100 mM TEAB) to 100 µL of sample (<1
143 µg/µL) for 1 h at 55°C. 2 µL of fresh alkylation buffer (625 mM iodoacetamide) was added to each sample and

144 incubated for 30 min at room temperature, in the dark. Following evaporation by SpeedVac, the samples were
145 resolubilized in 95 µL of 100 mM TEAB and sonicated for 10 min. The samples were treated with 2 µg of MS-
146 approved trypsin (Serva) for 18 h at 37°C. The reaction was stopped with 10 µL of 10% (v/v) formic acid and
147 again evaporated using the SpeedVac. Peptides were resolubilized in 25 µL 0.05% (v/v) TFA in 2/98 ACN/H_2O
148 (v/v) and sonicated for 15 min in a water bath before transfer to a 10 kDa molecular weight cut-off filter. After
149 15 min of centrifugation at 14,000 × *g* (20°C), the samples were transferred to HPLC vials and stored at -20°C.
150
151 **LC-MS/MS analysis.** LC-MS/MS analysis of trypsin-shaved surface peptides (method #1 and #2) and tryptic
152 peptides of secreted proteins (method #3) was performed on an Ultimate 3000 RSLC nano instrument coupled
153 to either a QExactive Plus (M#1 and M#3) or an HF (M#2) mass spectrometer (both Thermo Fisher Scientific) as
154 described previously [16]. Tryptic peptides were trapped for 4 min on an Acclaim Pep Map 100 column (2 cm ×
155 75 µm, 3 µm) at a flow-rate of 5 µL/min. The peptides were then separated on an Acclaim Pep Map column (50
156 cm × 75 µm, 2 µm) using a binary gradient (A: 0.1% (v/v) formic acid in H2O; B: 0.1% (v/v) formic acid in 90:10
157 (v/v) ACN/H2O).: M#1: 0-4 min at 4% B, 10 min at 7% B, 40 min at 10% B, 60 min at 15% B, 80 min at 25% B, 90
158 min at 35% B, 110 min at 50% B, 115 min at 60% B, 120-125 min at 96% B, 125.1-150 min at 4 % B. M#2: 0-4 min
159 at 4% B, 5 min at 8% B, 20 min at 12% B, 30 min at 18% B, 40 min at 25% B, 50 min at 35% B, 57 min at 50% B,
160 62-65 min at 96% B, 65.1-90 min at 4% B. M#3: 0-5 min at 4% B, 30 min at 7% B, 60 min at 10% B, 100 min at
161 15% B, 140 min at 25% B, 180 min at 45% B, 200 min at 65% B, 210-215 min at 96% B, 215.1-240 min at 4% B.
162 Positively charged ions were generated by a Nanospray Flex Ion Source (Thermo Fisher Scientific) using a
163 stainless steel emitter with 2.2 kV spray voltage. Ions were measured in Full MS / dd MS2 (Top10) mode, *i.e.*
164 precursors were scanned at m/z 300-1500 (R: 70,000 FWHM (M#1/#3)/: 60,000 FWHM (M#2); AGC target:
165 1·106e6; max. IT: 120 ms (M#1/#3) / 100 ms (M#2)). Fragment ions generated in the HCD cell at 30% normalized
166 collision energy using N2 were scanned (R: 17,500 FWHM (M#1/#3) / 15,000 FWHM (M#2); AGC target: 2e5;
167 max. IT: 120 ms (M#1/#3) / 100 ms (M#2)) in a data-dependent manner (dynamic exclusion: 30 s).

168

169 **Database search and data analysis of trypsin-shaved surface peptides.** The MS/MS data were searched against
170 the *A. fumigatus* Af293 genome of the *Aspergillus* Genome Database (AspGD); Uniprot Proteome ID
171 UP000000724 for *P. rubens*; Uniprot Proteome ID UP000077248 for *A. alternata*; and the Joint Genome Institute
172 MycoCosm annotation against the proteome of the related organism *C. fulvum* (described in [28, 29]) for *C.*
173 *herbarum*, using Proteome Discoverer 1.4 and 2.2 and the algorithms of Mascot 2.4.1, Sequest HT, and MS
174 Amanda as described previously [16]. Briefly, we allowed for two missed cleavages for tryptic peptides, a
175 precursor mass tolerance set to 10 ppm, and a fragment mass tolerance set to 0.02 Da. The dynamic
176 modification was set as oxidation of Met. For secretome analysis (method #3) the static modification was set to
177 carbamidomethylation of Cys. In all cases, at least 2 peptides per protein and a strict target false discovery (FDR)
178 rate of < 1% were required for positive protein hits.

179

180 **Data availability**

181 The mass spectrometry proteomics data have been deposited to the ProteomeXchange Consortium via the
182 PRIDE partner repository [30] with the dataset identifier PXD017067.

183

184 **Genetic manipulation of *A. fumigatus*.** All oligonucleotides utilized in this study are listed in **Table S2.** The
185 genetic deletions of *cweA* (Afu4g09600) and *scwA* (Afu4g09310) were generated using a 3-fragment PCR
186 method, as previously described [31]. ScwA, a small protein, was recently reannotated in *A. fumigatus* CEA10 as
187 indicated in **Figure S1A** (V. Valiante, personal communication). For the knockout constructs, flanking regions of
188 ~1 kb were amplified for each gene using *A. fumigatus* CEA17 genomic DNA as template and the appropriate
189 primer pairs (p1/p2 and p3/p4; **Figure S1B, C**). The pyrithiamine resistance marker (*ptrA*) was amplified from the
190 pSK275 plasmid using primers ptrA-F/R. Using Phusion polymerase (Thermo Scientific) and equimolar amounts
191 of the three fragments as template, primers p1 and p4 directed amplification of the entire construct (**Figure**

192 **S1D**). Knockouts of *A. fumigatus* were generated by homologous recombination following the transformation of
193 protoplasts [32]. Knockouts were verified by PCR and Southern blot according to standard procedures as
194 described below (**Figure S1E, F**).

195 Complemented strains were produced by knocking in the gene of interest to the endogenous locus of
196 the corresponding knockout strain (**Figure S1G-J**). Constructs were produced by fusion PCR using primers listed
197 in **Table S2**. Briefly, to complement strains CEA17Δ*scwA and* CEA17Δ*cweA*, plasmids *pUC19_scwA*c and
198 *pUC19_cweAc* were produced and transformed into protoplasts as previously described [32]. Both plasmids
199 were generated using a Gibson cloning and assembly kit (BioLabs) according to the manufacturer's instructions.
200 For *pUC19_scwAc*, the DNA fragments were generated as follows: the *scwA* gene and its 3' flanking region were
201 PCR amplified using primers scwA_F/scwA_hph_R and scwA_hph_F/scwA_R, respectively. The hygromycin
202 resistance cassette (*hph*) was amplified from the *pJWx41* plasmid with primers hph_scwA_F/hph_scwA_R, and
203 the plasmid *pUC19* backbone was amplified by PCR using primers pUC19_F/pUC19_R. The construct from
204 transformation was amplified using primer pair scwA_F and scwA_R. For *pUC19_cweA*c, the *cweA* gene and its 3'
205 flanking region were PCR amplified using primers cweA_F/cweA_hph_R and cweA_hph_F/cweA_R, respectively.
206 The hygromycin resistance cassette (*hph*) was amplified from *pJWx41* plasmid with primers
207 hph_cweA_F/hph_cweA_R, and the plasmid *pUC19* backbone was amplified by PCR using primers
208 pUC19_F/pUC19_R. Primer pair cweA_F/cweA_R was used for amplification of the construct for transformation.
209

210 **Southern blot analysis.** Southern blots to validate genetic deletion were carried out according to standard
211 protocols [33]. All sequence information was obtained from the Ensembl Fungi Database [34]. Genomic DNA of
212 *A. fumigatus* was isolated using the MasterPure Yeast DNA Purification Kit (Epicentre). Genomic DNA of *A.*
213 *fumigatus* was digested with the appropriate restriction enzymes (New England Biolabs). DNA fragments were
214 separated on an agarose gel followed by blotting onto Hybond N+ nylon membranes (GE Healthcare Bio-
215 Sciences). DNA probes using primers listed in **Table S2** were labeled with digoxigenin (DIG), hybridized in DIG

216 Easy Hyb, and detected using CDP-Star ready-to-use kit (Roche Applied Science), according to the
217 manufacturers' recommendations. Chemiluminescence signals were detected by a Fusion-FX CCD camera
218 (Vilbert Lourmat).
219
220 **Growth Assays of *A. fumigatus* knockouts.** Wild-type and knockout conidia were collected in water from AMM
221 agar plates after 5 days of growth. Conidia were counted using a CASY® Cell Counter (Omni Life Science), diluted
222 in droplet solution (0.9% (v/v) NaCl, 0.1% (v/v) Agar, 0.01% (v/v) Tween 20) and added to plates in 5 µL drops
223 containing 10^2, 10^3, 10^4, or 10^5 conidia. Growth was monitored over time at 37°C and images were collected
224 before overgrowth of the plate. Cell stress was induced using caffeine, caspofungin, calcofluor white, congo red,
225 and SDS at the designated concentrations. Germination assays were performed as above by microscopically
226 determining the ratio of spores undergoing germination (germ-tube formation) at each time point.
227
228 **Bioinformatic analyses.** Phylogenetic analyses were preformed using sequences gathered from FungiDB [35] for
229 each ortholog of *A. fumigatus* CweA and ScwA. Additional protein-protein BLAST (blastp) searches were
230 performed to confirm the collection of all orthologs. Alignments and phylogenetic trees were then produced
231 using the DNAStar MegAlign software package (DNASTAR Inc., USA) using a ClustalW alignment.
232 The InParanoid algorithm was used to identify ortholog clusters for pairwise species comparison [36].
233 The default algorithm parameters were used: a score cut-off of 40 bits, an overlap cut-off of 50%, and a segment
234 cut-off of 25%. The proteins with an ortholog score <0.95 contained in the ortholog clusters were excluded from
235 the analysis. "One to many" and "many to many" orthologous relationships were included in the ortholog
236 clusters. An ortholog group among 3 or 4 species was found only if the ortholog group was identified for all the
237 pairings. Furthermore, the InParanoid-defined ortholog clusters with at least one expressed protein were also
238 identified.
239

240 **Results and Discussion**

241 **The *A. fumigatus* surface proteome is dynamic across germination.**

242 In this study, we sought to expand the repertoire of *A. fumigatus* conidial surface and secreted proteins that
243 potentially trigger allergy or promote infection and compare the proteins exposed on the surface of *A.*
244 *fumigatus* conidia with other important allergenic molds. Initially, we utilized a previously-described trypsin-
245 shaving proteomics approach [16] to identify surface-exposed proteins throughout germination of the
246 filamentous fungus, *A. fumigatus* strain CEA10 (**Figure 1A**). Samples were collected from resting (0 h) conidia
247 grown at 37°C on AMM agar plates, and swollen conidia (5 h), germlings (8 h), and hyphae (14 h) germinated at
248 37°C in RPMI liquid media. We identified 177 unique proteins across all germination conditions. 75/177 proteins
249 had a predicted signal peptide cleavage site using the SignalP program [37], 15/177 contained at least one
250 predicted transmembrane helix (TMHMM), and 13/177 contained putative GPI anchors using PredGPI (**Table S3**;
251 [38]). When compared to previous trypsin-shaving data from the literature, 43/55 proteins from CEA10 were
252 found on the surface of *A. fumigatus* strain D141 resting conidia under comparable growth conditions, whereas
253 in swollen conidia, 98/139 CEA10 proteins were on the surface of D141 swollen conidia (**Figure 1B-C**; [16]).
254 These results suggest that the surface proteome of different *A. fumigatus* strains exhibit high similarities under
255 standard growth conditions. The surface proteins identified have a diverse array of cellular localizations and
256 activities using Gene Ontology Enrichment (fungidb.org). These include localization to the cell wall (72/177;
257 GO:0005618), cytoplasm (71/177; GO: 0005737), and external encapsulating structure (72/177; GO:0030312)
258 with activities related to catalytic activity (89/177; GO:0003824), binding (78/177; GO:0005488), oxidoreductase
259 activity (22/177; GO:0016491), and nucleic acid binding activity (16/177; GO:0003676), among others.

260 Over the course of germination, 55 proteins were identified on resting conidia (see **Table 1** for Top 20),
261 140 on swollen conidia, 56 on germlings, and 109 on hyphae. In direct comparisons between samples, 34
262 proteins were found in all four stages of the germination time course, including the conidial hydrophobin, RodA
263 (**Figure 2**). Somewhat surprisingly, RodA exhibited the highest levels of normalized abundance throughout

264 germination; ranging from 16.8% to 7.7% of the normalized peptide spectrum matches (PSMs) per length. As
265 confirmed by light microscopy (data not shown), the majority of conidia underwent germination in our assays;
266 however, a small fraction of conidia failed to germinate, which likely contributed to the abundance of RodA at
267 later time points.

268 In addition to RodA, the other most prevalent proteins on the surface of resting conidia, as determined
269 using normalized spectral abundance factor (NSAF; [39, 40]), were the protein of unknown function, ConJ,
270 Afu6g14470, and Afu2g05635; the serine protease, DppV; and the previously described surface protein CcpA.
271 Con-J shows high similarity to the conidiation-specific, light-induced protein 10 of *Neurospora crassa* and its
272 transcripts are upregulated during early conidial development and murine infection with *A. fumigatus* [18].
273 Afu6g14470 and Afu2g05635 remain relatively unstudied, but each contains a signal peptide cleavage site
274 according to SignalP [37] and Afu6g14470 was previously detected by 2D-gel electrophoresis on the conidial
275 surface of *A. fumigatus* [17]. The protein DppV is a secreted dipeptidyl-peptidase and nonclassical serine
276 protease [41], which is known to be targeted by the T cell response in mice surviving *A. fumigatus* infection [42].
277 The surface of swollen conidia exposed more proteins (140 unique proteins identified) than what was found on
278 the surface of the other time points, which is consistent with previous studies comparing resting and swollen
279 conidia [16]. It is possible that reorganization of the conidial surface during germination results in the temporary
280 availability of cell wall proteins to trypsin cleavage in some circumstances. The surface proteome of germlings
281 was less complex, with no proteins unique to only germlings, suggesting that perhaps there is a restriction to the
282 surface proteome in germlings. In hyphae, we again see slightly higher numbers of surface-exposed proteins,
283 with 30 proteins found that were not identified in the other samples (**Figure 2**).

284

285 **Knockout of abundant conidial surface proteins does not alter surface proteome.**

286 We were interested in further studying several of the more highly abundant surface proteins from *A.*
287 *fumigatus*. The putative GPI-anchored cell wall protein CweA (Afu4g09600, 980 amino acids) and the protein

288 ScwA (Afu4g09310, 93 amino acids) were both predicted to encode a signal peptide for entry into the secretory
289 pathway (SignalP), but otherwise lacked recognizable conserved domains or characterized orthologs. In addition
290 to being highly abundant, CweA and ScwA were observed on the surface throughout germination by trypsin
291 shaving (**Table S3**) and were previously found on the conidial surface in other studies [16, 43]. Interestingly,
292 *cweA* contains multiple coding tandem repeats, and its transcript was shown to be up-regulated upon
293 membrane stress [44].

294 Since ScwA is such a small protein, we first confirmed the annotation of the genetic loci in the CEA10
295 genome by multi-sequence alignment to related organisms after a resequencing of CEA10 *scwA* (**Figure S1A**).
296 ScwA appears to exclusively belong to a small subset of the *Aspergillus* genus (**Figure S2A**), while CweA is widely
297 found in both the *Aspergillus* and *Penicillium* genera (**Figure S2B**), with an ortholog expressed in *P. rubens*.
298 Genetic deletions of *cweA* (Afu4g09600) and *scwA* (Afu4g09310) were produced in *A. fumigatus* CEA17 by
299 homologous recombination following transformation of protoplasts (**Figure S1B-F).** Both knockouts grew
300 normally on AMM and malt agar plates (**Figure S3A**). The genetic deletion of *cweA* provided a growth advantage
301 relative to wild type on Congo Red agar plates, a known cell wall stressor, whereas Δ*scwA* exhibited only a minor
302 growth inhibition (**Figure 3A**). This finding is consistent with data from the literature showing that *cweA* was
303 downregulated in response to Congo Red stress [44]. Under calcofluor white stress, the Δ*scwA* strain exhibited a
304 slight advantage, whereas Δ*cweA* exhibited a more robust growth advantage, all of which could be
305 complemented (**Figure 3A**). Challenge with other cell wall and membrane stressors, including caffeine,
306 caspofungin, and SDS revealed no obvious defects by droplet assay (**Figure S3B**). Taken together, these results
307 suggest that the abundant surface proteins ScwA and CweA are important for fine tuning the conidial response
308 to stress.

309 Our previous characterization of the surface protein CcpA revealed an altered conidial surface proteome
310 after growth on AMM agar plates [16]. In this case, it was postulated that CcpA functions to mask other cell wall
311 proteins that are normally hidden in the conidial cell wall. To explore if other cell wall protein knockouts resulted

312 in a similar alteration to the surface proteome, we performed trypsin-shaving on the Δ*cweA* and Δ*scwA*
313 knockout strains. In both cases, we saw very little change to the exposed surface proteome, suggesting that the
314 function of CcpA in masking surface-exposed proteins is not a common feature of all abundant surface proteins,
315 but rather a specific feature of CcpA (**Table S4**; **Figure 3B**). Ultimately, these results suggest that the cell wall is
316 quite robust and adaptable, as even the removal of abundant cell surface proteins like CweA and ScwA yield few
317 major phenotypes. Further study will be required to fully understand the redundancy of conidial surface
318 proteins in cell wall maintenance and stress response.
319
320 **Growth temperature dictates the surface proteome of *A. fumigatus* conidia.**
321 As described above, the surface proteome undergoes dynamic changes during the germination process.
322 Previous studies showed that environmental conditions during conidiation affect the stress tolerance of *A.*
323 *fumigatus* conidia [45]. We thus wanted to understand if and how the temperature during conidiation influences
324 the surface proteome of *A. fumigatus* resting conidia. We performed trypsin-shaving proteomics on resting
325 conidia grown for 7 days at room temperature, 37°C, or 42°C and for 14 days at room temperature or 37°C.
326 Surprisingly, conidia produced at room temperature and 42°C had more surface-exposed proteins than spores
327 grown at 37°C after 7 days of growth (**Figure 4A**, **Table S5**). After 14 days of incubation, conidia grown at room
328 temperature and at 37°C both exhibited far fewer proteins on the surface, 19 and 29, respectively (**Figure 4B,**
329 **Table S5**). These results suggest that the surface proteome of conidia is potentially restricted or degraded over
330 developmental time. In corroboration with this idea of a surface proteome restriction is previous work showing
331 that the whole conidial proteome has a lower complexity at 15 days compared to conidia after 3 or 30 days of
332 growth [46]. It remains unclear how changes to the intracellular proteome might influence the surface proteome
333 during conidial development.
334 Interestingly, the ScwA protein appears to be only on the surface of conidia grown at 37°C, and not
335 room temperature, suggesting a possible role in temperature adaptation. However, we see no obvious growth

336 difference for the knockout strain at 37°C or room temperature. Five proteins were identified on resting conidia
337 grown at all tested time points and temperatures (**Table 2**), including one previously uncharacterized protein,
338 Afu8g01980. Overall, these results have obvious implications for the study of *A. fumigatus* pathogenesis and
339 reaffirm that the growth temperature of conidia can have a drastic effect on surface protein expression [45].
340 One partial explanation for the observed temperature-dependent effects is the difference in growth rate of *A.*
341 *fumigatus* on agar plates at room temperature and 37°C, where sporulation requires several additional days at
342 room temperature. At 14 days of incubation the conidia are mature under both conditions, and at this time
343 point we observe a similar number of proteins on the surface of conidia (**Figure 4B**). Despite a comparable
344 number of surface proteins, 19 for spores grown at room temperature and 29 for spores cultivated at 37°C, the
345 composition of the surface proteome is not the same at 14 days (10 shared proteins), suggesting some
346 temperature-dependent regulation of surface-exposed proteins.
347
348 **Comparative proteomics uncovers proteins on the surface/shed from allergenic fungal conidia.**
349 To refine our understanding of the surface-exposed cell wall proteins that might contribute to the
350 initiation of allergic inflammation in the lung, we leveraged the power of comparative proteomics. To this end,
351 the surface-exposed proteomes of 7-day-old resting conidia of *A. fumigatus* (CEA10) and three other prevalent
352 allergy-inducing fungi, *A. alternata* (ATCC 66981), *C. herbarum* (ATCC MYA-4682), and *P. rubens* (ATCC 28089)
353 grown at room temperature were assessed by trypsin-shaving proteomics. We first confirmed that the short
354 trypsin treatment yielded minimal cell lysis in all cases for resting conidia by staining with the cell-impermeable
355 dye propidium iodide (**Figure S4**). *A. alternata* and *C. herbarum* conidial populations contained a noticeable
356 fraction of dead cells, which were permeable to propidium iodide in both the presence and absence of trypsin
357 (**Figure S4**). Therefore, we believe that these datasets provide more information about trypsin-accessible
358 proteins (and likely immune-accessible proteins), and less information about the exact surface composition of *A.*
359 *alternata* and *C. herbarum*. Unfortunately, an annotated genome of *C. herbarum* is not available, so we relied on

360 the mapping of peptides to the annotated *C. fulvum* genome for these analyses, which potentially results in the
361 omission of some *C. herbarum*-specific surface proteins.

362 LC-MS/MS analysis revealed 252 surface-exposed proteins on resting conidia of *A. fumigatus*, 473 on *A.*
363 *alternata*, 240 on *C. herbarum*, and 254 on *P. rubens* (**Figure 5A**; **Table S6-S9**). On swollen conidia, we observed
364 49 surface-exposed proteins on *A. fumigatus*, 1,007 on *A. alternata*, 121 on *C. herbarum*, and 672 on *P. rubens*.
365 *A. fumigatus* conidia harvested from cultures grown at room temperature again exhibited more proteins on the
366 surface than conidia obtained from cultures grown at 37°C (**Figure 5B**). These results are also consistent with
367 previous studies that link fungal growth variability to cultivation temperature [45], and again highlight the
368 importance of selecting appropriate and consistent growth conditions. Interestingly, we observed conidia from
369 mycelia grown at room temperature or 37°C for 7 days responded differently to germination in RPMI, such that
370 swollen conidia exhibited vastly different surface proteomes after 5 hours at 37°C (**Figure 5C**). In particular,
371 swollen conidia grown initially at room temperature responded by restricting their surface proteomes, whereas
372 conidia grown initially at 37°C expanded their surface proteomes. The mechanism of this phenotype remains
373 unknown, but provides an interesting view of the dynamics of the surface proteome.

374 In addition to surface-exposed proteins, we were also interested in proteins secreted from swollen
375 conidia that may serve as immune modulators. Our previous proteomics analyses revealed an abundance of
376 proteins available for trypsin cleavage on swollen conidia. To test the hypothesis that a subset of these newly
377 surface-exposed proteins might also be secreted or shed from conidia, we performed solid-phase extraction of
378 spent cell culture supernatant after 5 h of germination. Using this method we were able to identify 371
379 *A. fumigatus* proteins secreted/shed after 5 h of incubation, 1,676 from *A. alternata*, 280 from *C. herbarum*, and
380 709 from *P. rubens* (**Figure 5A**, **Table S6-S9**). These findings highlight that many proteins exposed on the surface
381 of germinating *A. fumigatus* conidia are also secreted/shed into the local environment, where they may serve as
382 potential immune modulators to activate or inhibit host responses. In fact, 13 allergens were identified in *A.*
383 *fumigatus*, including the known *A. fumigatus* allergens, Asp f 1, Asp f 9, and Asp f 12. Of these 13 allergens, 9

384 were found only secreted/shed during swelling, two specific to resting conidia (Asp f 12, Asp f 23), and one from
385 all three conditions (Asp f 1). Three known allergens were identified in *A. alternata*, with two on the surface of
386 resting and swollen conidia as well as secreted/shed from swelling conidia (Alt a 6, Alt a 7), and one found only
387 secreted/shed from swelling conidia (Alt a 1). Four allergens were identified in analyses of *P. rubens*:
388 Pc20g10360 (Beta-hexosaminidase), Pc21g16950 (transaldolase), and Pc21g16970 (vacuolar serine proteinase)
389 were found on resting conidia, swollen conidia, and secreted/shed from swelling conidia; and the protein of
390 unknown function Pc12g10650 was found only secreted/shed from swelling conidia.
391
392 **Ortholog analysis reveals a conserved surface proteome among allergenic fungi**
393 Next, we used the InParanoid software package to assign ortholog groups between the different fungi in
394 our comparative proteomics datasets [36, 47]. The aim was to identify proteins that were conserved across all
395 four organisms as well as to define proteins that were specific to one organism. We were able to identify 125
396 orthologous surface/secreted protein groups detected in all four organisms (**Table 3**, **Table S10**). In *A. fumigatus*,
397 these orthologs corresponded mostly to proteins in the cytosol (91/125; GO:0005737), but a small subset was
398 found in the extracellular region (37/125; GO:0005576) by Gene Ontology Enrichment (fungidb.org). The large
399 number of proteins from the cytosol is indicative of the prevalent contamination of the cellular surface with
400 proteins from the intracellular space by each of the four tested fungi. Many represent ribosomal proteins,
401 chaperones, and metabolic enzymes, some of which have been shown to exhibit antigenic activity [48]. It is
402 possible that some of these proteins have moonlighting functions in the extracellular environment, as has been
403 observed in other systems [5]. For example, Asp F22 (enolase) was recently shown to bind human plasma
404 complement proteins to damage epithelial cell layers [49]. Interestingly, 42 *A. fumigatus* proteins were detected
405 in this experiment that had no ortholog in the related allergy-inducing species, including the Asp f 1 allergen.
406 102 proteins were specific to the extracellular space of *P. rubens*, 206 proteins unique to *A. alternata*, and 9 to

407 *C. herbarum* (**Table S10**). Of note, we did observe the *P. rubens* orthologs of *A. fumigatus* CweA and CcpA on *P.*
408 *rubens* conidia, perhaps suggesting a conserved function for these proteins in *P. rubens*.

409 Rapid detection and diagnosis of fungi, specifically fungal pathogens, remains a major hurdle in
410 managing allergic responses and invasive fungal disease. The ortholog analysis presented here provides
411 numerous candidate proteins likely accessible to both the immune system and potential diagnostic assays. Our
412 comparative proteomics approach and ortholog comparison also revealed that much overlap exists between *A.*
413 *fumigatus* and other allergy-inducing fungi, further complicating the development of future diagnostics and
414 highlighting the issue of cross-reactivity between organisms. The dynamic nature of the surface proteome of
415 fungi adds an additional complexity to this challenging problem. Despite these hurdles, we hope that the
416 datasets assembled here will serve as a resource in guiding future endeavors into the biology of the conidial
417 surface and selection of diagnostic targets, particularly in regard to antibody-based detection and chimeric
418 antigen receptor T cell-based therapeutics, which are proving to be more versatile in combatting infectious
419 diseases [50].

420

421 **Conclusions**

422 The surface of fungal conidia is a dynamic meshwork of macromolecules, including both glycans and proteins. In
423 this study, we identified the surface-exposed proteome of resting conidia from several allergenic fungal
424 pathogens and searched for orthologs between these organisms. We find that the surfaces of germinating fungi
425 are quite variable, which creates unique challenges for the identification of these organisms during allergy and
426 infection and further confirms that these fungi have sophisticated ways of managing diverse environments. In
427 fact, we show that temperature has a great effect on the surface proteome of *A. fumigatus*, a factor which must
428 be considered in the design of future experiments. We were able to significantly add to our collective knowledge
429 of the surface proteome of allergenic fungi in the early stages of germination and now have a resource that will
430 aid in the design of future diagnostics and therapeutics.

431

432 **Acknowledgements**

433 We would like to thank Laura Broschat for excellent technical assistance and Antje Häder for her assistance in

434 creating the Δ*cweA* knockout strain. We would also like to thank Vito Valiante for providing an updated gene

435 annotation for *scwA* and Volker Schwartze for thoughtful discussions throughout this project. We thank Amelia

436 Barber for critical reading of this manuscript. MGB was funded by the EXASENS project 13N13861. This work was

437 supported by the Deutsche Forschungsgemeinschaft (DFG)-funded Collaborative Research Center/Transregio

438 124 FungiNet (projects A1, B5 and Z2) and the DFG-funded ANR project AfuInf. The authors declare no conflicts

439 of interest.

440

441 **Tables**

442 **Table 1. Top 20 *A. fumigatus* proteins identified on resting conidia ranked by normalized spectral abundance**

443 **factor.**

Accession Number	Protein Name	NSAF	Description
Afu5g09580	RodA	0.126	Conidial hydrophobin
Afu6g03210	ConJ	0.093	Uncharacterized protein
Afu2g09030	DppV	0.055	Secreted dipeptidyl-peptidase
Afu6g14470	Afu6g14470	0.045	Uncharacterized protein
Afu2g05635	Afu2g05635	0.041	Uncharacterized protein
Afu1g13670	CcpA	0.040	Conidial cell wall protein
Afu4g09310	Afu4g09310	0.037	Uncharacterized protein
Afu4g09280	Afu4g09280	0.033	Uncharacterized protein
Afu5g14210	Grg1	0.033	Glucose-repressible gene
Afu1g14560	MsdS	0.030	Putative 1,2-alpha-mannosidase
Afu8g01980	Afu8g01980	0.027	Uncharacterized protein
Afu5g03540	Afu5g03540	0.024	Putative flavin-linked sulfhydryl oxidase activity
Afu2g17530	Abr2	0.023	Laccase
Afu8g05020	NagA	0.022	Putative secreted N-acetylhexosaminidase
Afu3g07160	Afu3g07160	0.020	Putative family 18 chitinase
Afu2g00680	Afu2g00680	0.020	Uncharacterized protein
Afu1g13550	Afu1g13550	0.019	Uncharacterized protein
Afu4g09600	Afu4g09600	0.018	Putative glycophosphatidylinositol (GPI)-anchored cell wall protein
Afu4g01290	Csn	0.016	Glycosyl hydrolase family 75 chitosanase
Afu5g09240	Sod1	0.016	Cu/Zn superoxide dismutase

444

445

446

447 **Table 2. *A. fumigatus* proteins identified on resting conidia at all tested time points and temperatures.**

Accession Number	Protein Name	Description
Afu5g09580	RodA	Conidial hydrophobin
Afu1g07440	Hsp70	Molecular chaperone
Afu8g01980	Afu8g01980	Uncharacterized protein
Afu2g17530	Abr2	Laccase
Afu1g05630	Afu1g05630	40S ribosomal protein S3, putative

448

449 **Table 3. Ortholog analysis on surface/secreted proteins of allergy-inducing fungi grown at room temperature.**

450 **(See also Table S10 in the supplements)**

Organism A	Organism B	Organism C	Organism D	Total Ortholog Groups from detected proteins	Ortholog Groups w/ orthologs detected in all organisms
A. fumigatus	*P. rubens*	*C. herbarum*	*A. alternata*	1617	125
A. fumigatus	*P. rubens*	*C. herbarum*	-	1050	134
A. fumigatus	*P. rubens*	-	*A. alternata*	1773	289
A. fumigatus	-	*C. herbarum*	*A. alternata*	1589	146
-	*P. rubens*	*C. herbarum*	*A. alternata*	1657	258
A. fumigatus	*P. rubens*	-	-	1146	351
A. fumigatus	-	*C. herbarum*	-	664	156
A. fumigatus	-	-	*A. alternata*	1737	377
-	*P. rubens*	-	*A. alternata*	1835	726
-	*P. rubens*	*C. herbarum*	-	992	276
-	-	*C. herbarum*	*A. alternata*	1739	359

451

452 **Figure Legends**

453 **Figure 1.** Trypsin-shaving proteomics of allergy-inducing fungi. A) Model of trypsin-shaving proteomics approach

454 to identifying surface-exposed peptides. Scaled Venn diagrams produced using the Biovenn software [51] show

455 intersection of proteins identified by trypsin shaving of B) resting and C) swollen conidia from *A. fumigatus* strain

456 CEA10 with D141 (D141 data described in [16]).

457

458 **Figure 2.** Trypsin shaving proteomics elucidates surface proteome of germinating conidia. 4-way comparison
459 indicating the intersection of surface-exposed proteins from resting and swollen conidia, germlings, and hyphae.
460 Plot produced using the R package UpSet.

461

462 **Figure 3.** Phenotypic analysis of conidial surface proteins. A) Droplet assays for growth of wild-type, Δ*cweA*, and
463 Δ*scwA* knockout strains grown on 35 µg/mL Congo red or 50 µg/mL calcofluor white. B) Scaled Venn diagram
464 indicating intersection of surface proteins identified by trypsin shaving of wild-type, Δ*cweA*, and Δ*scwA* knockout
465 strains.

466

467 **Figure 4.** Temperature influences the *A. fumigatus* surface proteome. A) Scaled Venn diagrams show the
468 intersection of proteins identified by trypsin shaving on the surface of resting conidia after A) 7 days or B) 14
469 days at 37°C or room temperature.

470

471 **Figure 5.** Comparative analysis reveals conserved surface proteins. A) Scaled Venn diagrams show the
472 intersection of surface-exposed proteins of resting conidia, swollen conidia (5 h), and extracellular proteins (5 h)
473 from *A. fumigatus*, *P. rubens*, *A. alternata*, and *C. herbarum*. B) Scaled Venn diagrams indicate difference in
474 surface proteome between resting conidia isolated from mycelia grown at room temperature or 37°C. C) Scaled
475 Venn diagrams indicate difference in surface proteome between swollen conidia isolated from mycelia grown at
476 room temperature or 37°C.

477

478 **References**

479 1. Hawksworth DL, Lucking R. Fungal Diversity Revisited: 2.2 to 3.8 Million Species. Microbiol Spectr.
480 2017;5(4). Epub 2017/07/29. doi: 10.1128/microbiolspec.FUNK-0052-2016. PubMed PMID: 28752818.
481 2. Simon-Nobbe B, Denk U, Poll V, Rid R, Breitenbach M. The spectrum of fungal allergy. Int Arch Allergy
482 Immunol. 2008;145(1):58-86. Epub 2007/08/22. doi: 10.1159/000107578. PubMed PMID: 17709917.

3. Fukutomi Y, Taniguchi M. Sensitization to fungal allergens: Resolved and unresolved issues. Allergol Int. 2015;64(4):321-31. Epub 2015/10/05. doi: 10.1016/j.alit.2015.05.007. PubMed PMID: 26433528.

4. Kousha M, Tadi R, Soubani AO. Pulmonary aspergillosis: a clinical review. Eur Respir Rev. 2011;20(121):156-74. doi: 10.1183/09059180.00001011. PubMed PMID: 21881144.

5. Blango MG, Kniemeyer O, Brakhage AA. Conidial surface proteins at the interface of fungal infections. PLoS Pathog. 2019;15(9):e1007939. Epub 2019/09/13. doi: 10.1371/journal.ppat.1007939. PubMed PMID: 31513678.

6. Dagenais TR, Keller NP. Pathogenesis of *Aspergillus fumigatus* in Invasive Aspergillosis. Clin Microbiol Rev. 2009;22(3):447-65. doi: 10.1128/CMR.00055-08. PubMed PMID: 19597008; PubMed Central PMCID: PMCPMC2708386.

7. Pollmacher J, Timme S, Schuster S, Brakhage AA, Zipfel PF, Figge MT. Deciphering the Counterplay of *Aspergillus fumigatus* Infection and Host Inflammation by Evolutionary Games on Graphs. Sci Rep. 2016;6:27807. doi: 10.1038/srep27807. PubMed PMID: 27291424; PubMed Central PMCID: PMCPMC4904243.

8. Mircescu MM, Lipuma L, van Rooijen N, Pamer EG, Hohl TM. Essential role for neutrophils but not alveolar macrophages at early time points following *Aspergillus fumigatus* infection. J Infect Dis. 2009;200(4):647-56. doi: 10.1086/600380. PubMed PMID: 19591573; PubMed Central PMCID: PMCPMC2745295.

9. Denning DW. Invasive aspergillosis. Clin Infect Dis. 1998;26(4):781-803; quiz 4-5. PubMed PMID: 9564455.

10. Bacher P, Heinrich F, Stervbo U, Nienen M, Vahldieck M, Iwert C, et al. Regulatory T Cell Specificity Directs Tolerance versus Allergy against Aeroantigens in Humans. Cell. 2016;167(4):1067-78 e16. Epub 2016/10/25. doi: 10.1016/j.cell.2016.09.050. PubMed PMID: 27773482.

11. de Ana SG, Torres-Rodriguez JM, Ramirez EA, Garcia SM, Belmonte-Soler J. Seasonal distribution of *Alternaria*, *Aspergillus*, *Cladosporium* and *Penicillium* species isolated in homes of fungal allergic patients. J Investig Allergol Clin Immunol. 2006;16(6):357-63. PubMed PMID: 17153883.

12. Caillaud D, Leynaert B, Keirsbulck M, Nadif R, mould Awg. Indoor mould exposure, asthma and rhinitis: findings from systematic reviews and recent longitudinal studies. Eur Respir Rev. 2018;27(148). Epub 2018/05/18. doi: 10.1183/16000617.0137-2017. PubMed PMID: 29769295.

13. Bozek A, Pyrkosz K. Immunotherapy of mold allergy: A review. Hum Vaccin Immunother. 2017;13(10):2397-401. doi: 10.1080/21645515.2017.1314404. PubMed PMID: 28481693; PubMed Central PMCID: PMCPMC5647975.

14. Bowyer P, Denning DW. Genomic analysis of allergen genes in *Aspergillus* spp: the relevance of genomics to everyday research. Med Mycol. 2007;45(1):17-26. doi: 10.1080/13693780600972907. PubMed PMID: 17325940.

15. Baltussen TJH, Zoll J, Verweij PE, Melchers WJG. Molecular Mechanisms of Conidial Germination in Aspergillus spp. Microbiol Mol Biol Rev. 2020;84(1). Epub 2019/12/06. doi: 10.1128/MMBR.00049-19. PubMed PMID: 31801804.

16. Voltersen V, Blango MG, Herrmann S, Schmidt F, Heinekamp T, Strassburger M, et al. Proteome Analysis Reveals the Conidial Surface Protein CcpA Essential for Virulence of the Pathogenic Fungus *Aspergillus fumigatus*. MBio. 2018;9(5). doi: 10.1128/mBio.01557-18. PubMed PMID: 30279286.

17. Asif AR, Oellerich M, Amstrong VW, Riemenschneider B, Monod M, Reichard U. Proteome of conidial surface associated proteins of Aspergillus fumigatus reflecting potential vaccine candidates and allergens. J Proteome Res. 2006;5(4):954-62. Epub 2006/04/11. doi: 10.1021/pr0504586. PubMed PMID: 16602703.

18. Suh MJ, Fedorova ND, Cagas SE, Hastings S, Fleischmann RD, Peterson SN, et al. Development stage-specific proteomic profiling uncovers small, lineage specific proteins most abundant in the *Aspergillus fumigatus* conidial proteome. Proteome Sci. 2012;10(1):30. doi: 10.1186/1477-5956-10-30. PubMed PMID: 22545825; PubMed Central PMCID: PMCPMC3424117.

530 19. Cagas SE, Jain MR, Li H, Perlin DS. The proteomic signature of *Aspergillus fumigatus* during early
531 development. Mol Cell Proteomics. 2011;10(11):M111 010108. doi: 10.1074/mcp.M111.010108. PubMed PMID:
532 21825280; PubMed Central PMCID: PMCPMC3226407.
533 20. Erwig LP, Gow NA. Interactions of fungal pathogens with phagocytes. Nat Rev Microbiol. 2016;14(3):163-
534 76. doi: 10.1038/nrmicro.2015.21. PubMed PMID: 26853116.
535 21. Paris S, Debeaupuis JP, Crameri R, Carey M, Charles F, Prevost MC, et al. Conidial hydrophobins of
536 *Aspergillus fumigatus*. Appl Environ Microbiol. 2003;69(3):1581-8. PubMed PMID: 12620846; PubMed Central
537 PMCID: PMCPMC150101.
538 22. Thau N, Monod M, Crestani B, Rolland C, Tronchin G, Latge JP, et al. rodletless mutants of *Aspergillus*
539 *fumigatus*. Infect Immun. 1994;62(10):4380-8. PubMed PMID: 7927699; PubMed Central PMCID:
540 PMCPMC303120.
541 23. Dague E, Alsteens D, Latge JP, Dufrene YF. High-resolution cell surface dynamics of germinating
542 *Aspergillus fumigatus* conidia. Biophys J. 2008;94(2):656-60. doi: 10.1529/biophysj.107.116491. PubMed PMID:
543 17890393; PubMed Central PMCID: PMCPMC2157220.
544 24. Kozel TR, Wickes B. Fungal diagnostics. Cold Spring Harb Perspect Med. 2014;4(4):a019299. Epub
545 2014/04/03. doi: 10.1101/cshperspect.a019299. PubMed PMID: 24692193; PubMed Central PMCID:
546 PMCPMC3968782.
547 25. Rhodes J. Rapid Worldwide Emergence of Pathogenic Fungi. Cell Host Microbe. 2019;26(1):12-4. Epub
548 2019/07/12. doi: 10.1016/j.chom.2019.06.009. PubMed PMID: 31295419.
549 26. Brakhage AA, Van den Brulle J. Use of reporter genes to identify recessive trans-acting mutations
550 specifically involved in the regulation of *Aspergillus nidulans* penicillin biosynthesis genes. J Bacteriol.
551 1995;177(10):2781-8. PubMed PMID: 7677843; PubMed Central PMCID: PMCPMC176949.
552 27. Maerker C, Rohde M, Brakhage AA, Brock M. Methylcitrate synthase from *Aspergillus fumigatus*.
553 Propionyl-CoA affects polyketide synthesis, growth and morphology of conidia. FEBS J. 2005;272(14):3615-30.
554 doi: 10.1111/j.1742-4658.2005.04784.x. PubMed PMID: 16008561.
555 28. de Wit PJ, van der Burgt A, Okmen B, Stergiopoulos I, Abd-Elsalam KA, Aerts AL, et al. The genomes of
556 the fungal plant pathogens *Cladosporium fulvum* and *Dothistroma septosporum* reveal adaptation to different
557 hosts and lifestyles but also signatures of common ancestry. PLoS Genet. 2012;8(11):e1003088. doi:
558 10.1371/journal.pgen.1003088. PubMed PMID: 23209441; PubMed Central PMCID: PMCPMC3510045.
559 29. Ohm RA, Feau N, Henrissat B, Schoch CL, Horwitz BA, Barry KW, et al. Diverse lifestyles and strategies of
560 plant pathogenesis encoded in the genomes of eighteen *Dothideomycetes* fungi. PLoS Pathog.
561 2012;8(12):e1003037. doi: 10.1371/journal.ppat.1003037. PubMed PMID: 23236275; PubMed Central PMCID:
562 PMCPMC3516569.
563 30. Perez-Riverol Y, Csordas A, Bai J, Bernal-Llinares M, Hewapathirana S, Kundu DJ, et al. The PRIDE
564 database and related tools and resources in 2019: improving support for quantification data. Nucleic Acids Res.
565 2019;47(D1):D442-D50. Epub 2018/11/06. doi: 10.1093/nar/gky1106. PubMed PMID: 30395289; PubMed
566 Central PMCID: PMCPMC6323896.
567 31. Szewczyk E, Nayak T, Oakley CE, Edgerton H, Xiong Y, Taheri-Talesh N, et al. Fusion PCR and gene
568 targeting in *Aspergillus nidulans*. Nat Protoc. 2006;1(6):3111-20. doi: 10.1038/nprot.2006.405. PubMed PMID:
569 17406574.
570 32. Weidner G, d'Enfert C, Koch A, Mol PC, Brakhage AA. Development of a homologous transformation
571 system for the human pathogenic fungus *Aspergillus fumigatus* based on the *pyrG* gene encoding orotidine 5'-
572 monophosphate decarboxylase. Curr Genet. 1998;33(5):378-85. PubMed PMID: 9618589.
573 33. Sambrook J, Russell DW. Molecular Cloning: A Laboratory Manual: Cold Spring Harbor Laboratory Press;
574 2001.
575 34. Howe KL, Contreras-Moreira B, De Silva N, Maslen G, Akanni W, Allen J, et al. Ensembl Genomes 2020-
576 enabling non-vertebrate genomic research. Nucleic Acids Res. 2019. Epub 2019/10/11. doi: 10.1093/nar/gkz890.
577 PubMed PMID: 31598706.

578 35. Basenko EY, Pulman JA, Shanmugasundram A, Harb OS, Crouch K, Starns D, et al. FungiDB: An Integrated
579 Bioinformatic Resource for Fungi and Oomycetes. J Fungi (Basel). 2018;4(1). Epub 2018/08/29. doi:
580 10.3390/jof4010039. PubMed PMID: 30152809; PubMed Central PMCID: PMCPMC5872342.
581 36. O'Brien KP, Remm M, Sonnhammer EL. Inparanoid: a comprehensive database of eukaryotic orthologs.
582 Nucleic Acids Res. 2005;33(Database issue):D476-80. Epub 2004/12/21. doi: 10.1093/nar/gki107. PubMed PMID:
583 15608241; PubMed Central PMCID: PMCPMC540061.
584 37. Nielsen H, Engelbrecht J, Brunak S, von Heijne G. Identification of prokaryotic and eukaryotic signal
585 peptides and prediction of their cleavage sites. Protein Eng. 1997;10(1):1-6. PubMed PMID: 9051728.
586 38. Pierleoni A, Martelli PL, Casadio R. PredGPI: a GPI-anchor predictor. BMC Bioinformatics. 2008;9:392.
587 doi: 10.1186/1471-2105-9-392. PubMed PMID: 18811934; PubMed Central PMCID: PMCPMC2571997.
588 39. Zybailov B, Mosley AL, Sardiu ME, Coleman MK, Florens L, Washburn MP. Statistical analysis of
589 membrane proteome expression changes in *Saccharomyces cerevisiae*. J Proteome Res. 2006;5(9):2339-47. doi:
590 10.1021/pr060161n. PubMed PMID: 16944946.
591 40. Florens L, Carozza MJ, Swanson SK, Fournier M, Coleman MK, Workman JL, et al. Analyzing chromatin
592 remodeling complexes using shotgun proteomics and normalized spectral abundance factors. Methods.
593 2006;40(4):303-11. doi: 10.1016/j.ymeth.2006.07.028. PubMed PMID: 17101441; PubMed Central PMCID:
594 PMCPMC1815300.
595 41. Beauvais A, Monod M, Wyniger J, Debeaupuis JP, Grouzmann E, Brakch N, et al. Dipeptidyl-peptidase IV
596 secreted by *Aspergillus fumigatus*, a fungus pathogenic to humans. Infect Immun. 1997;65(8):3042-7. PubMed
597 PMID: 9234752; PubMed Central PMCID: PMCPMC175429.
598 42. Beauvais A, Monod M, Debeaupuis JP, Diaquin M, Kobayashi H, Latge JP. Biochemical and antigenic
599 characterization of a new dipeptidyl-peptidase isolated from *Aspergillus fumigatus*. J Biol Chem.
600 1997;272(10):6238-44. PubMed PMID: 9045640.
601 43. Levdansky E, Kashi O, Sharon H, Shadkchan Y, Osherov N. The *Aspergillus fumigatus* cspA gene encoding
602 a repeat-rich cell wall protein is important for normal conidial cell wall architecture and interaction with host
603 cells. Eukaryot Cell. 2010;9(9):1403-15. doi: 10.1128/EC.00126-10. PubMed PMID: 20656913; PubMed Central
604 PMCID: PMCPMC2937338.
605 44. Levdansky E, Romano J, Shadkchan Y, Sharon H, Verstrepen KJ, Fink GR, et al. Coding tandem repeats
606 generate diversity in Aspergillus fumigatus genes. Eukaryot Cell. 2007;6(8):1380-91. Epub 2007/06/15. doi:
607 10.1128/EC.00229-06. PubMed PMID: 17557878; PubMed Central PMCID: PMCPMC1951137.
608 45. Hagiwara D, Sakai K, Suzuki S, Umemura M, Nogawa T, Kato N, et al. Temperature during conidiation
609 affects stress tolerance, pigmentation, and trypacidin accumulation in the conidia of the airborne pathogen
610 *Aspergillus fumigatus*. PLoS One. 2017;12(5):e0177050. doi: 10.1371/journal.pone.0177050. PubMed PMID:
611 28486558; PubMed Central PMCID: PMCPMC5423626.
612 46. Anjo SI, Figueiredo F, Fernandes R, Manadas B, Oliveira M. A proteomic and ultrastructural
613 characterization of Aspergillus fumigatus' conidia adaptation at different culture ages. J Proteomics.
614 2017;161:47-56. Epub 2017/04/04. doi: 10.1016/j.jprot.2017.03.021. PubMed PMID: 28365406.
615 47. Remm M, Storm CE, Sonnhammer EL. Automatic clustering of orthologs and in-paralogs from pairwise
616 species comparisons. J Mol Biol. 2001;314(5):1041-52. doi: 10.1006/jmbi.2000.5197. PubMed PMID: 11743721.
617 48. Teutschbein J, Simon S, Lother J, Springer J, Hortschansky P, Morton CO, et al. Proteomic Profiling of
618 Serological Responses to Aspergillus fumigatus Antigens in Patients with Invasive Aspergillosis. J Proteome Res.
619 2016;15(5):1580-91. Epub 2016/03/15. doi: 10.1021/acs.jproteome.6b00042. PubMed PMID: 26974881.
620 49. Dasari P, Koleci N, Shopova IA, Wartenberg D, Beyersdorf N, Dietrich S, et al. Enolase From Aspergillus
621 fumigatus Is a Moonlighting Protein That Binds the Human Plasma Complement Proteins Factor H, FHL-1, C4BP,
622 and Plasminogen. Front Immunol. 2019;10:2573. Epub 2019/12/12. doi: 10.3389/fimmu.2019.02573. PubMed
623 PMID: 31824478; PubMed Central PMCID: PMCPMC6883375.

624 50. Parida SK, Poiret T, Zhenjiang L, Meng Q, Heyckendorf J, Lange C, et al. T-Cell Therapy: Options for
625 Infectious Diseases. Clin Infect Dis. 2015;61Suppl 3:S217-24. Epub 2015/09/27. doi: 10.1093/cid/civ615. PubMed
626 PMID: 26409284; PubMed Central PMCID: PMCPMC4583575.
627 51. Hulsen T, de Vlieg J, Alkema W. BioVenn - a web application for the comparison and visualization of
628 biological lists using area-proportional Venn diagrams. BMC Genomics. 2008;9:488. doi: 10.1186/1471-2164-9-
629 488. PubMed PMID: 18925949; PubMed Central PMCID: PMCPMC2584113.

630

631 **Supplemental Figure Legends**

632 **Figure S1.** Production of Δ*cweA* and Δ*scwA* knockouts in *A. fumigatus*. A) Reannotation of *scwA* (Afu4g09310)
633 from *A. fumigatus* CEA10. For production of genetic deletions of B) *cweA* and C) *scwA* flanking DNA sequences
634 were amplified using the appropriate primers p1-p4. D) The flanking DNA sequences were then combined with
635 the *ptrA* resistance marker by Phusion polymerase and primers p1/4 to produce a construct with gene flanking
636 regions surrounding the resistance marker. Genetic deletions of E) *cweA* and F) *scwA* were then confirmed by
637 Southern blot analysis. Complemented strains for G) *cweA* and H) *scwA* were produced by introducing a
638 construct containing a 5' flanking sequence (F1), the gene with both 5' and 3' UTRs, a hygromycin resistance
639 cassette (*hph*), and a 3' flanking sequence (F2) into the original locus of the corresponding knockout strain *via*
640 homologous recombination. Southern blots were performed to confirm complementation of I) *cweA* and J)
641 *scwA*.

642

643 **Figure S2.** Phylogenetic analysis of *A. fumigatus* cell surface proteins. A) Phylogenetic tree of ScwA sequences
644 produced using the DNAStar MegAlign software with a ClustalW alignment of all sequences deemed significant
645 by NCBI Blastp suite. B) Phylogenetic tree of CweA sequences produced using the DNAStar MegAlign software
646 with a ClustalW alignment of all sequences deemed significant by NCBI Blastp suite.

647

648 **Figure S3.** Growth characterization of the Δ*cweA* and Δ*scwA* knockouts. A) Growth on AMM and malt agar plates
649 for 48 h. B) Strains were serially diluted and spotted onto AMM agar with the addition of the indicated stressors
650 and grown for 72 h. Experiments are representative data from three separate experiments.

651

652 **Figure S4.** Trypsin does not induce major changes in *A. fumigatus* conidial permeability. Images show

653 representative fungal conidia stained for 15 min with the cell-impermeable dye propidium iodide (red) following

654 treatment with 1% (w/v) SDS (left) or 5 µg/mL trypsin for 5 min at 37°C (right).

655

656 **Supplemental Tables**

657 **Table S1**. Fungal strains used in this study.

Strain	Genotype/Phenotype	Source
CEA10	*A. fumigatus* wild type	Fungal Genetics Stock Center (A1163)
CEA17	*A. fumigatus akuB*^{KU80} deletion in CEA10	Da Silva Ferreira et al., 2006
CEA17*Δ*cweA	Derived from CEA17; *Afu4g09600*::*ptrA*; PtrA^{R}, Δ*Afu4g09600*	This study
CEA17*Δ*cweA + CweA	*ΔcweA* complemented strain	This study
CEA17*ΔscwA*	Derived from CEA17; *Afu4g09310*::*ptrA*; PtrA^{R}, Δ*Afu4g09310*	This study
CEA17*ΔscwA* + ScwA	*ΔscwA* complemented strain	This study
ATCC 66981	*A. alternata* wild type	American Type Culture Collection
ATCC 28089	*P. rubens* wild type	American Type Culture Collection
ATCC MYA-4682	*C. herbarum* wild type	American Type Culture Collection

658

659 **Table S2**. Oligonucleotides and plasmids used in this study.

Oligonucleotide	Sequence (5'—3')	Target
Gene Deletion		
cweA-1	TAACAGAACCTGCCACGACC	*cweA*
cweA-2	GGCCTGAGTGGCCATCGAATTCTTCCTCCGACCAGACCCTTC	*cweA*
cweA-3	GAGGCCATCTAGGCCATCAAGCGCTGTCATTCGTGCCGTTGA	*cweA*
cweA-4	GCAAGCGCAGCAAGATAAGG	*cweA*
scwA-1	GCCCACATGCCTCTAGACTC	*scwA*
scwA-2	GGCCTGAGTGGCCATCGAATTCCGATCAGCACTCTGGTACTG	*scwA*
scwA-3	GAGGCCATCTAGGCCATCAAGCGGAGATGGCTGGATATAGTC	*scwA*
scwA-4	GCGAGAACCAGAGCGCAAAC	*scwA*
prtA-1	GAATTCGATGGCCACTCAGGCC	*ptrA*
prtA-2	GCTTGATGGCCTAGATGGCCTC	*ptrA*
Complementation		
scwA_F	TATCACGAGGCCCTTTCGTCAAGCAAGACCAGAACCTGAAATC	*scwA*
scwA_hph_R	GCTCCCCAGGGCTTCTAGTGGATATCTG	*scwA*

scwA_hph_F	GCAAAGGAATATGAAGGGCTTTCCCGAAAG	*scwA*
scwA_R	CATCGTCACCAACCACACGTCGCGCGTTTCGGTGATGAC	*scwA*
hph_scwA_F	GGGCTTCTAGTGGATATCTGCAGAATTCGC	*hph*
hph_scwA_R	GTCCGAGGGCAAAGGAATATGAAGGGCT	*hph*
pUC19_F	TCGCGCGTTTCGGTGATG	*pUC19*
pUC19_R	GTATCACGAGGCCCTTTCGTC	*pUC19*
cweA_F	TATCACGAGGCCCTTTCGTCCTAACAGAACCTGCCACG	*cweA*
cweA_hph_R	CTAGCTTACGAAGATCAAGAATTTCGCCAGTGTG	*cweA*
cweA_hph_F	CAAAGGAATAGTCAGCCATGTGTGGTCTC	*cweA*
cweA_R	CATGAGTTTATTAGGGAGCATGAGTCGCGCGTTTCGGTGATGAC	*cweA*
hph_cweA_F	TCAAGAATTTCGCCAGTGTGATGGATATC	*hph*
hph_cweA_R	GTCCGAGGGCAAAGGAATAGTCAGCCATG	*hph*
Plasmids	***Source***	
pUC19	New England Biolabs	
pUC19_scwAc	Complementation plasmid produced in this study	
pUC19_cweAc	Complementation plasmid produced in this study	

660

661 **Table S3.** Surface proteome of germinating *A. fumigatus* conidia (Excel File).

662 **Table S4.** Surface proteome of Δ*scwA* and Δ*cweA* deletion strains (Excel File).

663 **Table S5.** Temperature-dependent surface proteome of *A. fumigatus* conidia (Excel File).

664 **Table S6.** Surface proteome and secretome of resting and swollen *A. fumigatus* conidia (Excel File).

665 **Table S7.** Surface proteome and secretome of resting and swollen *P. rubens* conidia (Excel File).

666 **Table S8.** Surface proteome and secretome of resting and swollen *A. alternata* conidia (Excel File).

667 **Table S9.** Surface proteome and secretome of resting and swollen *C. herbarum* conidia (Excel File).

668 **Table S10.** Ortholog analysis performed using InParanoid software package (Excel File).

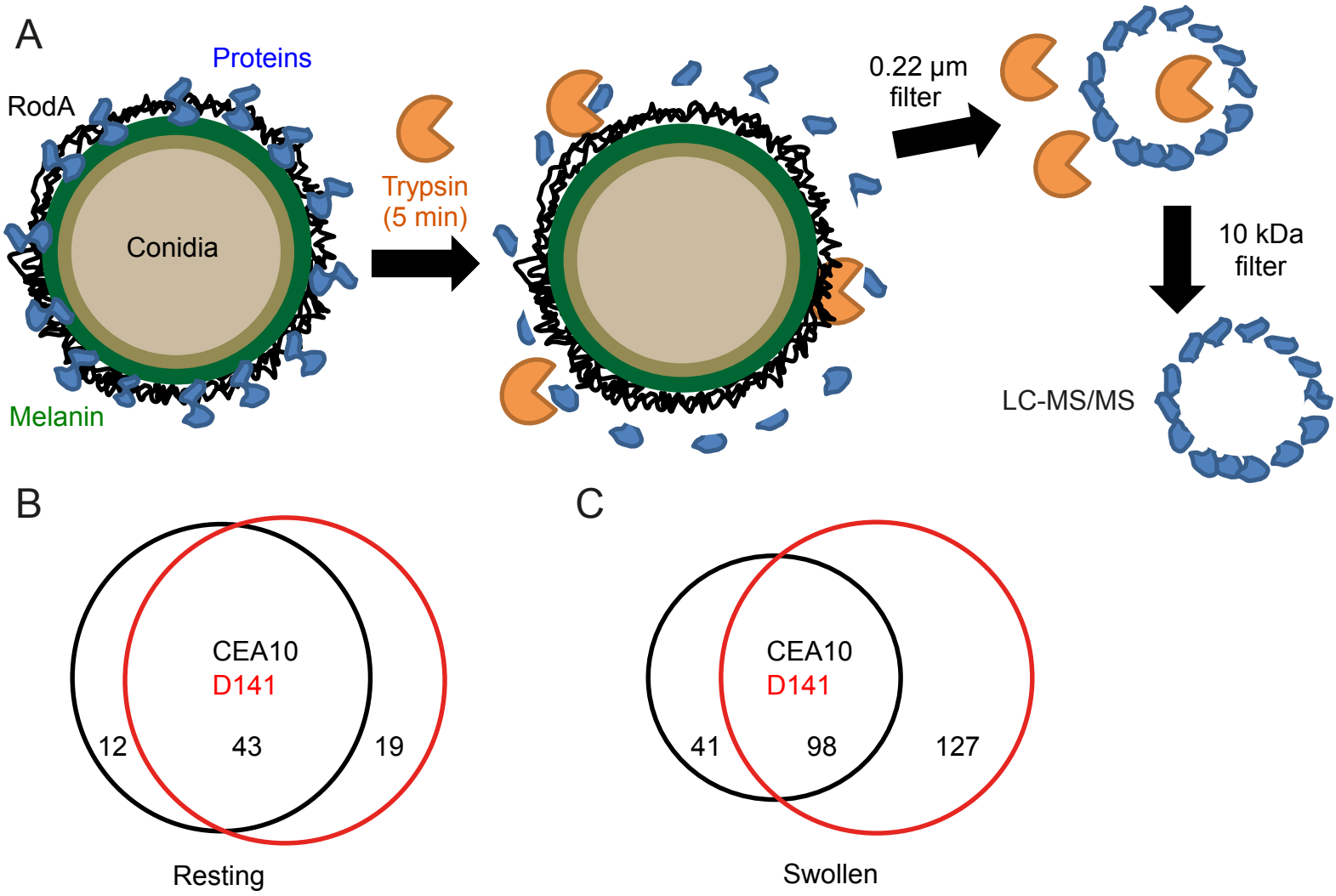
A
Proteins
RodA
Conidia
Melanin
Trypsin
(5 min)
0.22 µm
filter
10 kDa
filter
LC-MS/MS
B
CEA10
D141
12
43
19
Resting
C
CEA10
D141
41
98
127
Swollen

Figure 1

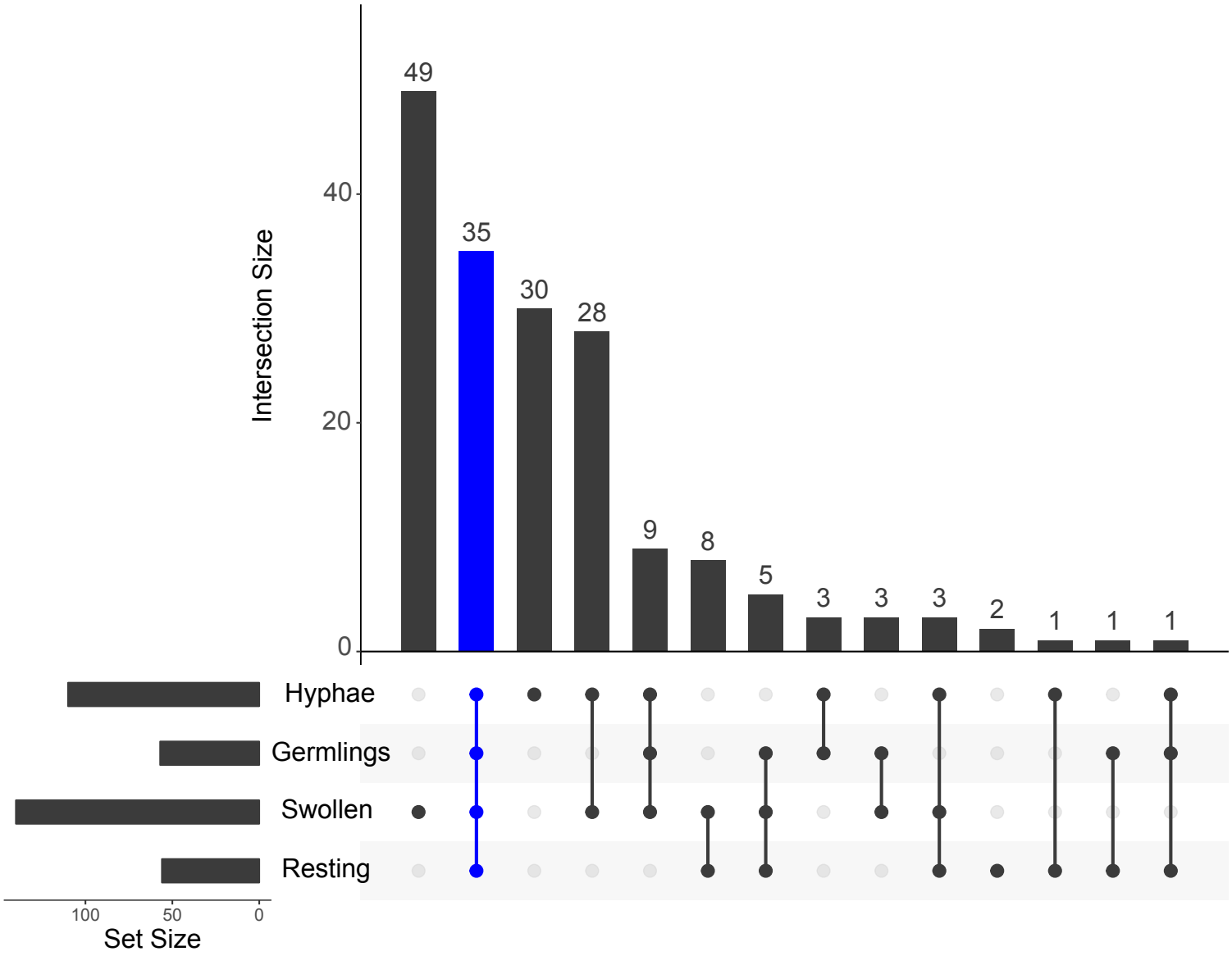
Intersection Size
0
20
40
49
35
30
28
9
8
5
3
3
3
2
1
1
1
Hyphae
Germlings
Swollen
Resting
100
50
0
Set Size

Figure 2

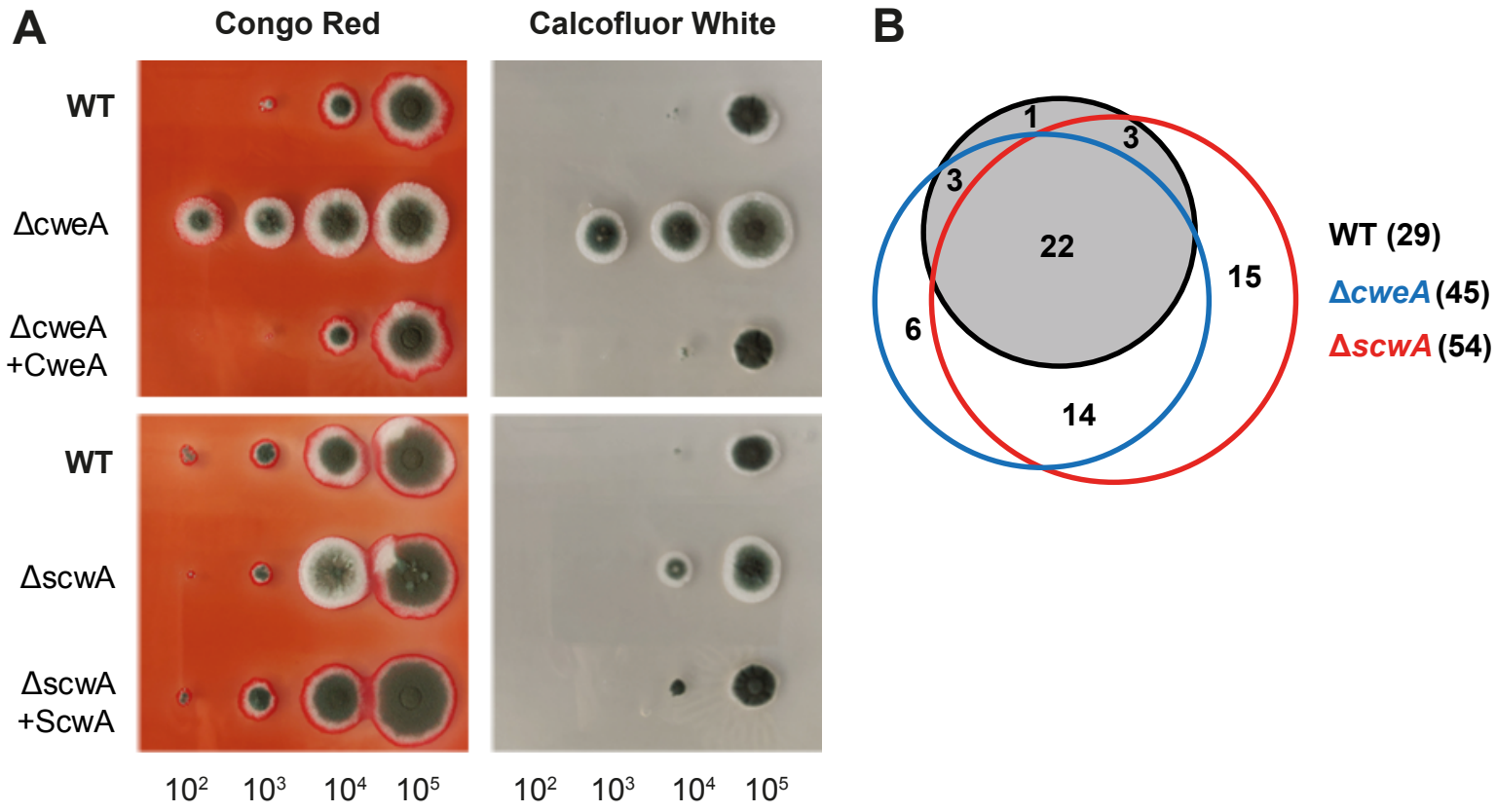
A
Congo Red
Calcofluor White
WT
ΔcweA
ΔcweA
+CweA
WT
ΔscwA
ΔscwA
+ScwA
10²
10³
10⁴
10⁵
10²
10³
10⁴
10⁵
B
1
3
3
22
15
6
14
WT (29)
ΔcweA (45)
ΔscwA (54)

Figure 3

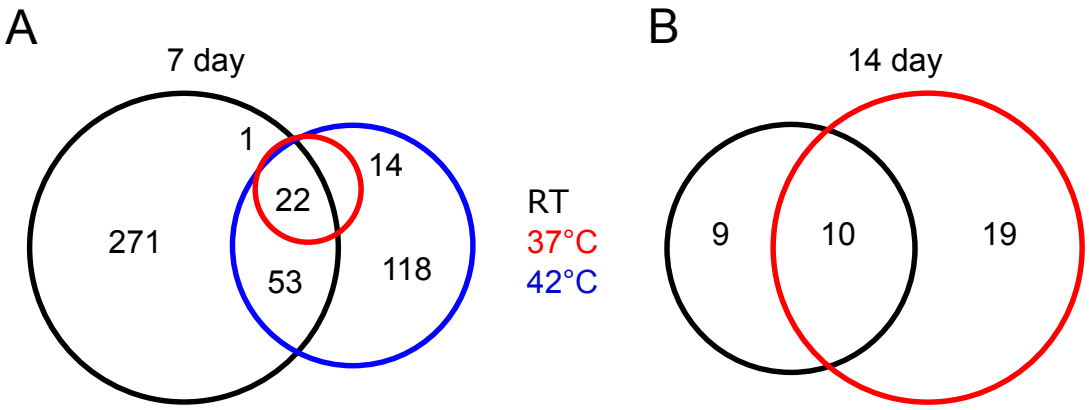

Figure 4

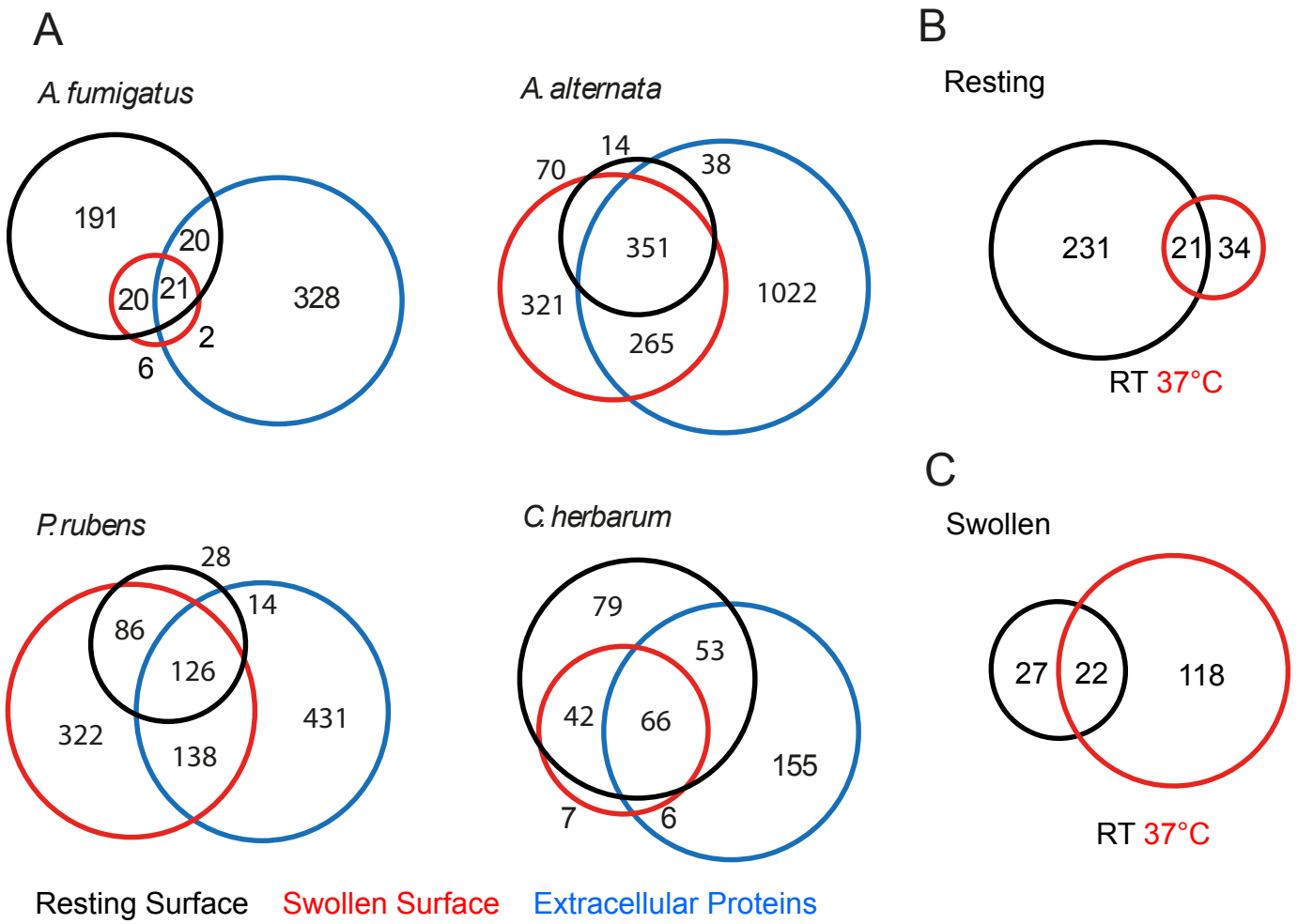
A
A. fumigatus
191
20
20
21
328
2
6
A. alternata
14
70
38
351
321
1022
265
B
Resting
231
21
34
RT 37°C
C
Swollen
27
22
118
RT 37°C
P. rubens
28
14
86
126
322
431
138
C. herbarum
79
53
42
66
155
7
6
Resting Surface
Swollen Surface
Extracellular Proteins

Figure 5

A

```
                                                          1                                                                                  80
Afu4g09310_A_fumigatus_Af293                    (1) ----------------------------------------MHDLYRFVDHAKSVDNALLFRRSTAPSFANQGIKGLNNR
AFUB_066440_A_fumigatus_A1163                   (1) MKAVPQCEIATRHPLLLRPNIRPCMISIDLLIMRSPLTTPYCKHARGTGLRASSRLSRRRFRRSTAPSFANQGIKGLNNR
ALT_5420_Aspergillus_lentulus                   (1) ------------------------------------------------------------------------------------
AUD_2568_Aspergillus_udagawae                   (1) ------------------------------------------------------------------------------------
NFIA_106700_Neosartorya_fischeri                (1) ------------------------------------------------------------------------------------
AFUB_hki_066490_(old_acc_AFUB_066440)_New_annotation (1) ------------------------------------------------------------------------------------
Y699_06317_Aspergillus_fumigatus_Z5             (1) ------------------------------------------------------------------------------------
Consensus                                       (1)

                                                          81                                                                                160
Afu4g09310_A_fumigatus_Af293                   (40) AWS-HHHHHHHHQRSFSPQHGLLISQAQLSDSNQLQNAVLYYPLPPRRCWHDHGCPFCRAYVSQPLQSNHPTNEPGRQSN
AFUB_066440_A_fumigatus_A1163                  (81) AWSHHHHHHHHHQRSFSPQHGLLISQAQLSDSNQLQNAVLYYPLPPRRCWHDHGCPFCRAYVSQPLQSNHPTNEPGRQSN
ALT_5420_Aspergillus_lentulus                   (1) ----------------------------------------------------MQFSTIVSLLAVAGMTVAAPSVARRQSN
AUD_2568_Aspergillus_udagawae                   (1) ----------------------------------------------------MQFSTIFSLLAVVGMTVAAPPVVHPQSN
NFIA_106700_Neosartorya_fischeri                (1) ----------------------------------------------------MQFSTILSLLAVAGMTVAVPSVARRQSN
AFUB_hki_066490_(old_acc_AFUB_066440)_New_annotation (1) ----------------------------------------------------MQFSTILSLLAVAGMTMAAPSVARRQSN
Y699_06317_Aspergillus_fumigatus_Z5             (1) ----------------------------------------------------MQFSTILSLLAVAGMTMAAPSVARRQSN
Consensus                                      (81)                                                         MQFSTILSLLAVAGMTVAAPSVARRQSN

                                                          161                                                                   230
Afu4g09310_A_fumigatus_Af293                  (119) HNGLAGVNVENNKIPVNVDVPIKGNNVANGVANDVLKDGVDVEHVAD-AVNAGVLGNANQVAPQGF----
AFUB_066440_A_fumigatus_A1163                 (161) HNGLAGVNVENNKIPVNVDVPIKGNNVANGVANDVLKDGVDVEHVAD-AVNAGVLGNANQVAPQGF----
ALT_5420_Aspergillus_lentulus                  (29) NNGLAGVNVEDTNVPVNVNVPIKGNNVANGVANGVLKDGVNVEHVAD-AVNAGVLGQANQVAPKGGLPPF
AUD_2568_Aspergillus_udagawae                  (29) KNGVVGLNVADTTVPVDVDVPIQGNNVADNVANGLLDGGVNLDHTVDGPLNVAALGKADQIAPKGALPPF
NFIA_106700_Neosartorya_fischeri               (29) NNGLAGVNLENTKIPVNVDVPIKGNNVANGVANDVLEDGVNVEHVAD-AVNAGVLGNANQVAPQGF----
AFUB_hki_066490_(old_acc_AFUB_066440)_New_annotation (29) HNGLAGVNVENNKIPVNVDVPIKGNNVANGVANDVLKDGVDVEHVAD-AVNAGVLGNANQVAPQGF----
Y699_06317_Aspergillus_fumigatus_Z5            (29) HNGLAGVNVENNKIPVNVDVPIKGNNVANGVANDVLKDGVDVEHVAD-AVNAGVLGNANQVAPQGF----
Consensus                                     (161) HNGLAGVNVENNKIPVNVDVPIKGNNVANGVANDVLKDGVDVEHVAD AVNAGVLGNANQVAPQGF
```

ScwA Predicted Protein Sequence

MQFSTILSLLAVAGMTMAAPSVARRQSNHNGLAGVNVENNKIPVNVDVPIKGNNVANGVAND
VLKDGVDVEHVADAVNAGVLGNANQVAPQGF

B

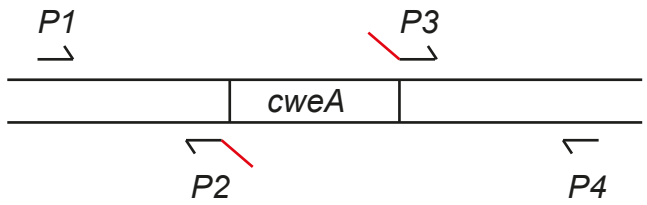

C

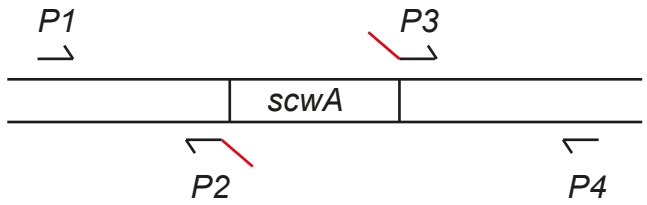

D

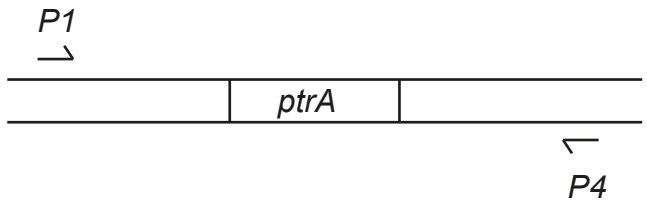

E

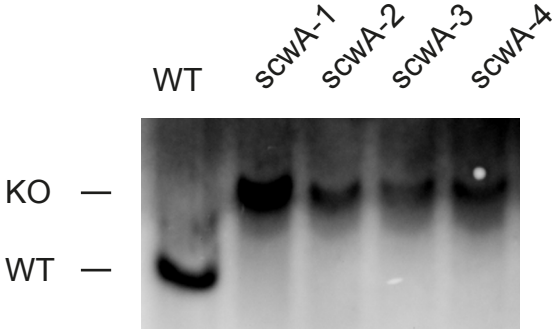

F

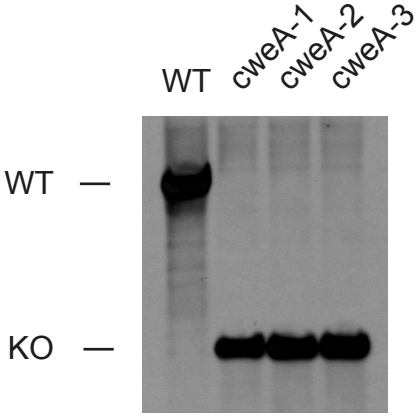

G

H

I

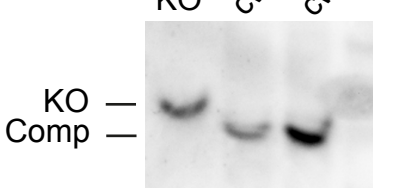

J

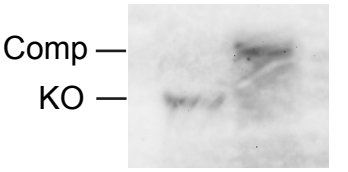

Figure S1

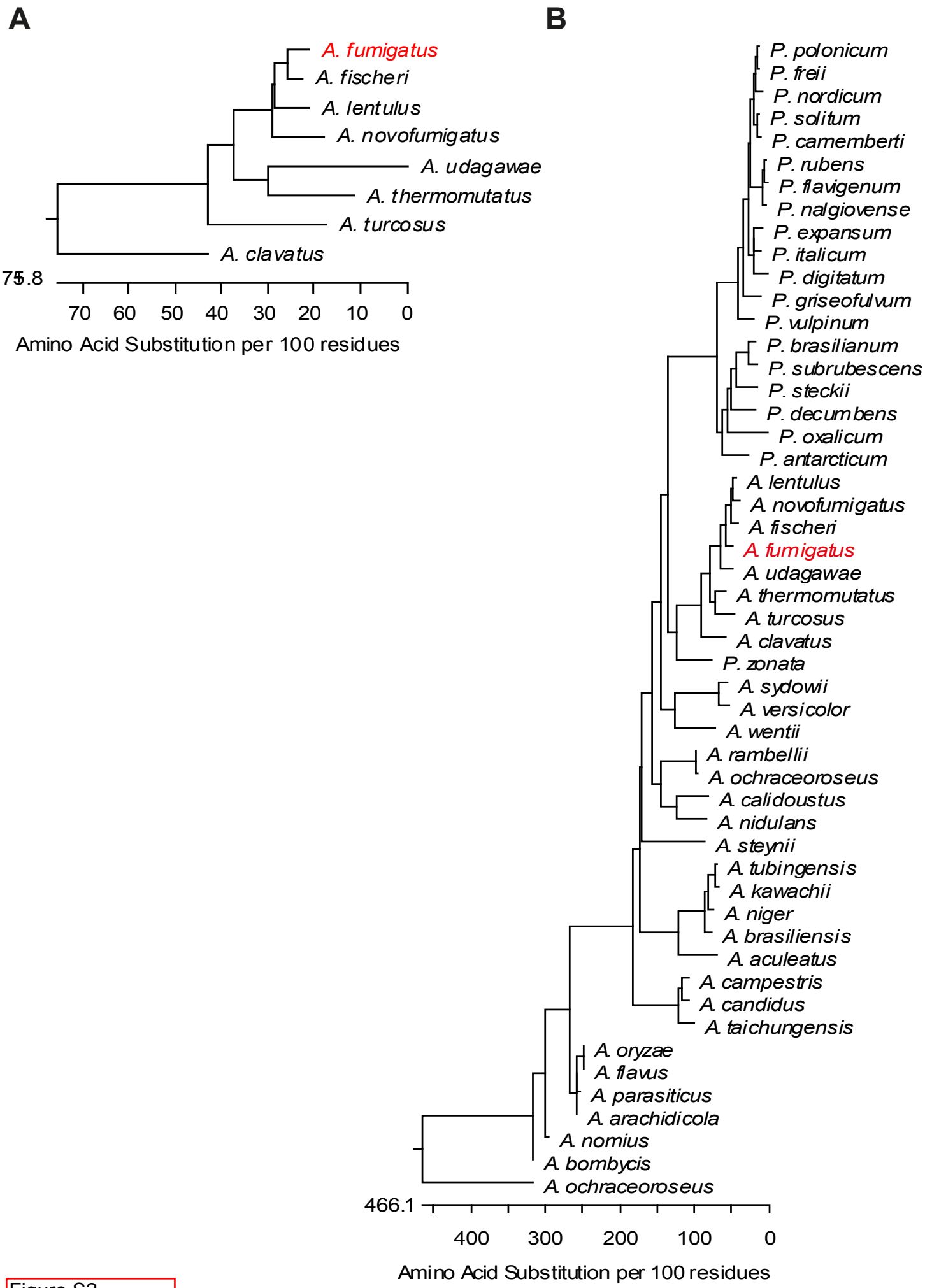
A
A. fumigatus
A. fischeri
A. lentulus
A. novofumigatus
A. udagawae
A. thermomutatus
A. turcosus
A. clavatus
75.8
70 60 50 40 30 20 10 0
Amino Acid Substitution per 100 residues
B
P. polonicum
P. freii
P. nordicum
P. solitum
P. camemberti
P. rubens
P. flavigenum
P. nalgiovense
P. expansum
P. italicum
P. digitatum
P. griseofulvum
P. vulpinum
P. brasilianum
P. subrubescens
P. steckii
P. decumbens
P. oxalicum
P. antarcticum
A. lentulus
A. novofumigatus
A. fischeri
A. fumigatus
A. udagawae
A. thermomutatus
A. turcosus
A. clavatus
P. zonata
A. sydowii
A. versicolor
A. wentii
A. rambellii
A. ochraceoroseus
A. calidoustus
A. nidulans
A. steynii
A. tubingensis
A. kawachii
A. niger
A. brasiliensis
A. aculeatus
A. campestris
A. candidus
A. taichungensis
A. oryzae
A. flavus
A. parasiticus
A. arachidicola
A. nomius
A. bombycis
A. ochraceoroseus
466.1
400 300 200 100 0
Amino Acid Substitution per 100 residues

Figure S2

A

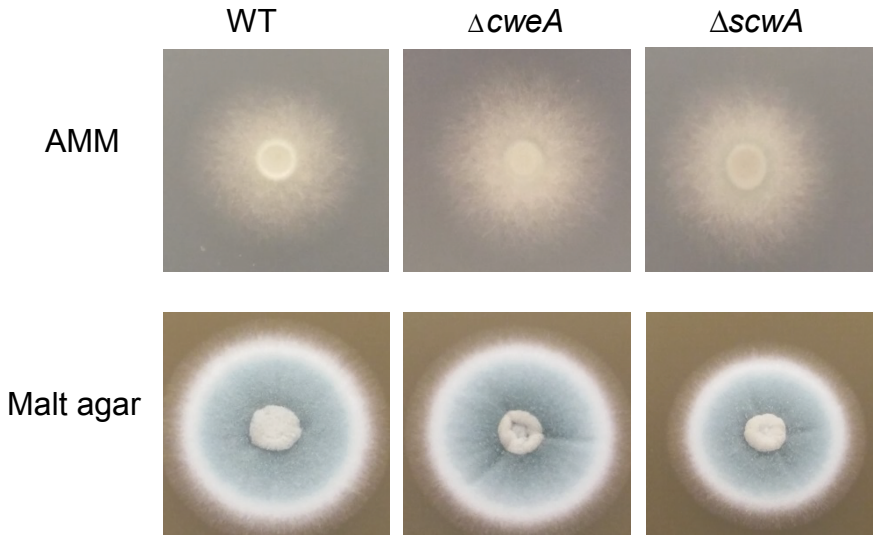
WT
ΔcweA
ΔscwA
AMM
Malt agar

B

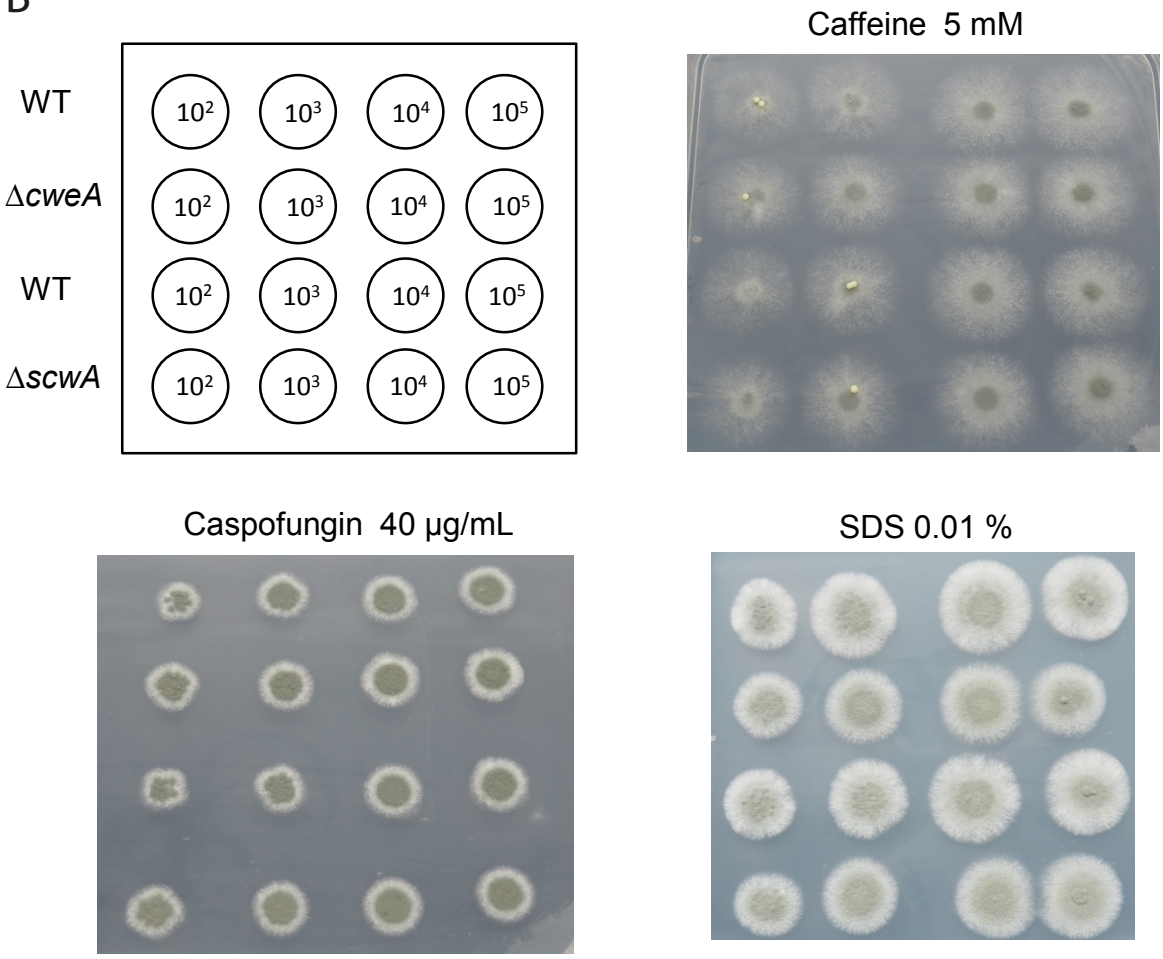
WT
ΔcweA
WT
ΔscwA
10²
10³
10⁴
10⁵
Caffeine 5 mM
Caspofungin 40 µg/mL
SDS 0.01 %

Figure S3

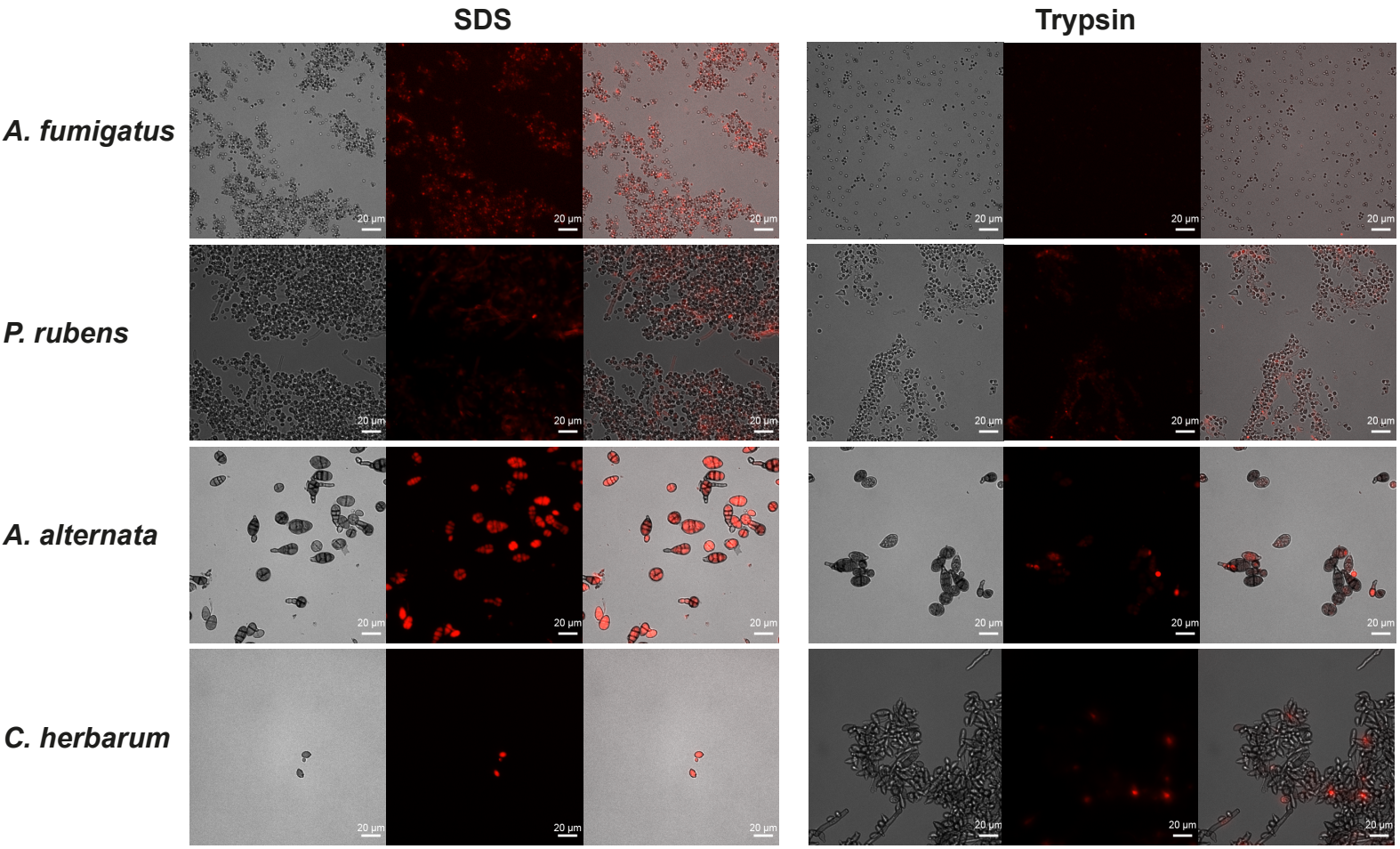
SDS
Trypsin
A. fumigatus
P. rubens
A. alternata
C. herbarum
20 µm

FIgure S4